INDIUM NITRIDE: A NEW MATERIAL FOR HIGH EFFICIENCY, COMPACT, 1550NM LASER-BASED TERAHERTZ SOURCES IN EXPLOSIVES DETECTION AND CONCEALED WEAPONS IMAGING

Michael Wraback*, Grace D. Chern, Eric D. Readinger, and Paul H. Shen
U.S. Army Research Laboratory, Sensors and Electron Devices Directorate, AMSRD-ARL-SE-EM
2800 Powder Mill Road, Adelphi, MD 20783

Gregor Koblmueller, Chad S. Gallinat, and James S. Speck
Materials Department, University of California Santa Barbara, CA 93106

William J. Schaff
Cornell University, 415 Phillips Hall, Ithaca, NY 14853

ABSTRACT

Indium nitride (InN) is identified as a promising terahertz (THz) emitter based on the optical and electronic properties of high quality In- and N-face samples. Time domain THz spectroscopy has been employed to measure the pump wavelength and background carrier concentration dependence of THz emission from InN. There is no discernable difference between the In- and N-face InN samples, as expected for the improved crystalline quality and concomitant low background electron density and high mobility for both polarities. While there is only a weak dependence of THz signal on pump wavelength from 800 nm to 1500 nm, there is a strong dependence on background electron density. Modeling shows that the dominant mechanism for THz generation in bulk InN is the current associated with the diffusion of the photo-generated electrons at elevated electron temperature (photo-Dember effect) and the redistribution of the background electrons under drift, with larger screening from the higher mobility electrons as compared to holes. Compensation or p-type doping in conjunction with manipulation of the large internal electric fields in InN/InGaN nanostructures should lead to significant improvements in THz emitters.

1. INTRODUCTION

The terahertz region of the electromagnetic spectrum, lying between microwave frequencies (100 GHz) and photonic frequencies (30 THz), is a potentially important region for important Army applications such as rapid identification of explosive devices (Barber et al., 2005, Shen et al., 2005), chemical and biological agents (Samuels et al., 1999, Markelz et al., 2000, Woolard et al., 2002, Globus et al., 2003, Liu et al., 2004), and identification/imaging of concealed objects and through obscurants (Federici et. al., 2005). In spite of its potential, the THz regime remains one of the least explored portions of the electromagnetic spectrum, in part because of the difficulty in efficiently generating and detecting terahertz radiation. There are two approaches to generating terahertz radiation that have found some success. One approach uses optical pulses of ~ 100 fs duration to produce broadband radiation from semiconductors via acceleration of photogenerated charge, dynamic field screening, optical rectification, or photo-Dember effect (Zhang et al., 1990, Turchinovich et al., 2003, Liu et al., 2006). Narrow band radiation can also be created through the mixing of quasi-CW lasers separated in frequency by the desired terahertz difference frequency in a semiconductor photomixer (Bjarnason et al., 2004). Traditionally, optically generated THz systems utilize femtosecond mode-locked Ti-sapphire lasers or CW lasers with a wavelength near 800 nm. Significant advantages associated with the use of telecommunications grade optoelectronics and compact fiber lasers could be gained in cost, size, weight, efficiency, and field deployability by shifting the wavelength to 1550 nm if an appropriate narrow bandgap semiconductor THz source were available.

With a bandgap below 0.7 eV (Wu et al., 2002, Gallinat et al., 2006, Koblmüller et al., 2006), InN is an attractive material amenable to 1550 nm phtoexcitation that has not been extensively explored for THz applications. Manipulation of the large internal electric fields in InN/InGaN nanostructures should enable one to far surpass the state-of-the-art in THz emitters. Unlike conventional III-V semiconductor compounds, III-V nitride semiconductors have a wurtzite crystal structure. Wurtzite is a polar structure that can support a significant spontaneous polarization even in the absence of any external field or strain. In InN/GaInN multiple quantum wells (MQWs), the termination of the spontaneous polarization at the well/barrier interfaces can lead to a large built-in electric field in InN that points in the growth direction. This internal field can be further enhanced by the piezoelectric field in the strained heterostructure, and

Report Documentation Page

Form Approved
OMB No. 0704-0188

1. REPORT DATE	2. REPORT TYPE	3. DATES COVERED
01 NOV 2006	**N/A**	**-**

4. TITLE AND SUBTITLE	5a. CONTRACT NUMBER
Indium Nitride: A New Material for High Efficiency, Compact, 1550 nm Laser-Based Terahertz Sources in Explosives Detection and Concealed Weapons Imaging	5b. GRANT NUMBER
	5c. PROGRAM ELEMENT NUMBER
6. AUTHOR(S)	5d. PROJECT NUMBER
	5e. TASK NUMBER
	5f. WORK UNIT NUMBER
7. PERFORMING ORGANIZATION NAME(S) AND ADDRESS(ES) **U.S. Army Research Laboratory, Sensors and Electron Devices Directorate, AMSRD-ARL-SE-EM 2800 Powder Mill Road, Adelphi, MD 20783**	8. PERFORMING ORGANIZATION REPORT NUMBER
9. SPONSORING/MONITORING AGENCY NAME(S) AND ADDRESS(ES)	10. SPONSOR/MONITOR'S ACRONYM(S)
	11. SPONSOR/MONITOR'S REPORT NUMBER(S)

12. DISTRIBUTION/AVAILABILITY STATEMENT
Approved for public release, distribution unlimited

13. SUPPLEMENTARY NOTES
See also ADM002075., The original document contains color images.

14. ABSTRACT

15. SUBJECT TERMS

16. SECURITY CLASSIFICATION OF:			17. LIMITATION OF ABSTRACT	18. NUMBER OF PAGES	19a. NAME OF RESPONSIBLE PERSON
a. REPORT	b. ABSTRACT	c. THIS PAGE			
unclassified	**unclassified**	**unclassified**	**UU**	**31**	

the combination of these effects is predicted to create fields about an order of magnitude larger than conventional III-V materials (Bernardini et al., 1997). For example, we have calculated that an $InN/Ga_{0.2}In_{0.8}N$ MQW with 2 nm well width will have a field greater than 2 MV/cm. While the THz radiation field is proportional to the number of photoexcited carriers under low excitation conditions, one can readily gauge the importance of the enhanced internal electric field by considering the MQW structure as a nanoscale capacitor, with the energy transfer from the excitation pulse to the THz pulse mediated by the partial or complete discharge of the nanocapacitor. Therefore the maximum THz pulse energy is limited by the electrostatic energy stored in the nanocapacitor, $U=1/2\ \varepsilon\varepsilon_0 AdF^2$, where $\varepsilon\varepsilon_0$ is the static permittivity, A is the area, d is the effective width of the capacitor, and F is the electric field inside the capacitor. This simple relation therefore shows that the large internal electric field in InN/GaInN MQWs should yield a significant enhancement in the efficiency of THz generation when the sample is excited by short optical pulses in the fs fiber laser spectral region (1550 nm, 1030 nm). In addition, for CW THz generation obtained from the mixing of two frequency offset CW lasers, 1550 nm operation is advantageous because the photomixing conversion factor $(e/h\nu)^2$ is about four times higher than it is at GaAs wavelengths (λ <850 nm). This result combined with the high saturation velocity (> 1.5 X 10^7cm/s) (Liang et al., 2004), large intervalley spacing (2.7 eV) to confine carriers within the high mobility gamma valley, short carrier lifetime, and potentially high breakdown voltage in InN should lead to up to an order of magnitude higher efficiency InN-based sources compared with the commonly employed arsenides.

In this paper, we report on the development of InN as a potential narrow bandgap semiconductor source of THz radiation under 1550 nm fs or CW laser excitation. The growth, optical, and electronic properties of optimized In- and N-face InN are presented. Femtosecond pulses tunable between 800 nm and 1500 nm are used to generate THz radiation from this optimized InN. These results are evaluated within the context of similar data obtained from p-InAs, the best known THz surface emitter, using drift-diffusion equations incorporating momentum conservation and relaxation.

2. GROWTH AND PROPERTIES OF HIGH QUALITY INDIUM NITRIDE

High quality In-face and N-face InN samples have been grown by plasma-assisted molecular beam epitaxy. The In-face InN samples were grown on Ga-polar GaN templates using GaN buffer layers grown in the Ga droplet regime, which significantly improved the surface morphology of the InN layers (Gallinat et al., 2006). The N-face InN samples were grown on free-standing N-face GaN or C-face 6H-SiC substrates (Koblmüller et al., 2006). Growth on the N-face exhibits higher thermal stability, with growth temperatures up to ~ 100° C higher than for In-face growth (Xu and Yoshikawa, 2003).

Unintentionally doped In-polar InN films have been realized with room temperature electron mobilities as high as 2900 cm^2/Vs and free electron concentrations as low as 2.3 x 10^{17} cm^{-3}. Figure 1 shows the optical

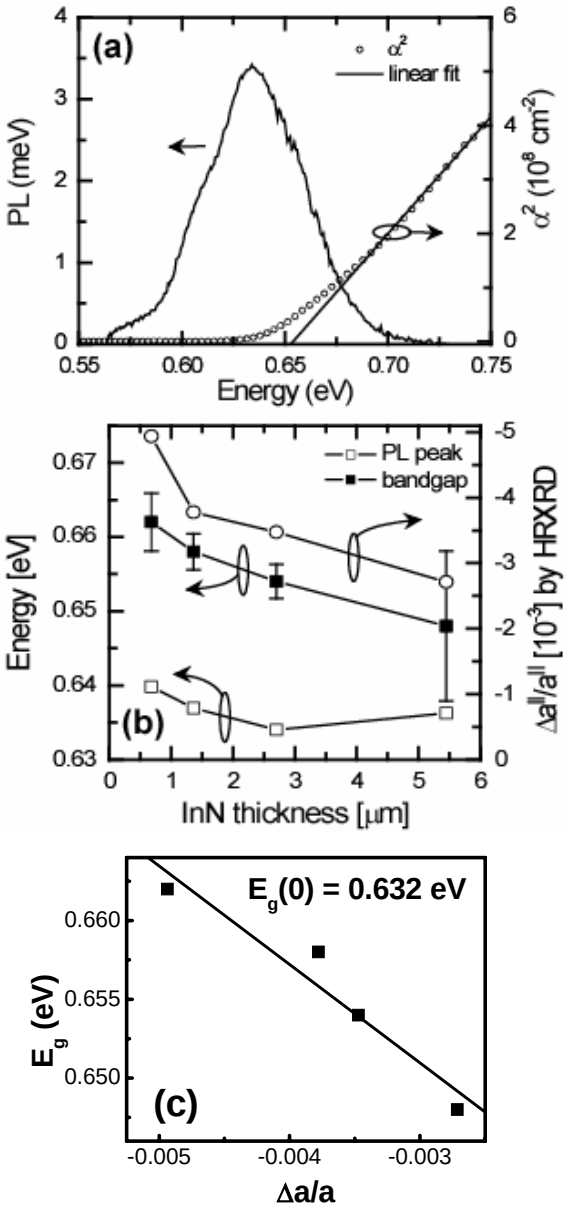

Fig. 1. (a) PL spectra and bandgap from fit to absorption data in InN; (b) Comparison of bandgap energy, peak PL emission energy and residual compressive strain as a function of InN thickness; (c) Extrapolation of bandgap to zero strain.

properties of an unintentionally doped InN thickness series evaluated at room temperature by CW reflectance, transmission, and photoluminescence (PL) measurements. The absorption coefficient was calculated from the reflectance and transmission data, and its square is plotted versus photon energy to determine the direct bandgap of the InN. Figure 1a shows representative results for a 2.7 μm thick sample. The intercept of the linear fit with the energy axis provides a bandgap of 0.654 ± 0.002 eV. The PL peak was Stokes-shifted by 20 meV to 0.634 eV, implying that the emission emanates substantially from the bandtail states. Figure 1b compares the bandgap obtained from the fit described above, the PL peak energy, and the residual compressive strain (as measured by HRXRD) for the InN film thickness series. The bandgap decreased from 0.662 ± 0.004 eV to 0.648 ± 0.01 eV as the film thickness increased from 0.68 to 5.45 μm, most likely due to the reduction in residual compressive strain. A similar shift in PL peak energy, from 0.64 eV to ~ 0.635 eV, is observed with increasing thickness. This shift may be less pronounced because the absorption depth of the 900 nm excitation laser is much smaller (~200-300 nm) than the thickness of most of the InN films. Figure 1c shows a linear fit to the relation between the bandgap and the strain. Extrapolation of the bandgap data to zero strain using the deformation potential for InN (4.1 eV) obtained from the slope of the line provides an unstrained bandgap of ~0.63 eV. Similar data has also been obtained on optimized N-face InN films. The electron mobility as high as 2370 cm^2/Vs is almost a factor of two higher and the corresponding bulk carrier concentration of 2.8×10^{17} cm^{-3} is nearly one order of magnitude lower than those reported for the best MBE grown N–face InN (Xu and Yoshikawa, 2003). Optical measurements provide a bandgap of 0.651 eV, with PL peak emission at 0.626 eV, both among the lowest reported values for N-face InN.

3. THZ EMISSION FROM HIGH QUALITY INDIUM NITRIDE

The THz measurements were performed using the experimental set-up shown in Fig. 2. The output of the Ti:sapphire regenerative amplifier (RegA) at 800 nm is split into two beams. The stronger beam is frequency doubled to serve as the pump source for an optical parametric amplifier, which generates a tunable infrared pulse (0.9–2.6 μm) in the idler beam. The infrared beam, after compression with a prism pair to typical pulse widths of approximately 150 fs, is then incident on the InN sample at 45° to the surface normal. The subsequent terahertz emission is collected with a pair of parabolic mirrors on to a ZnTe crystal for electro-optic sampling. The weaker RegA split-off beam is used to probe the terahertz emission for all excitation wavelengths, as well as to pump the InN samples at 800nm.

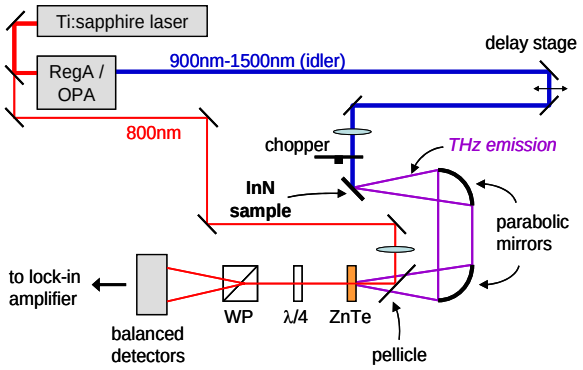

Fig.2. Experimental set-up for generation and detection of THz radiation.

Preliminary measurements of terahertz emission from InN thin films deposited on GaN buffers on sapphire using fs pulse excitation at 800 nm have been performed (Ascazubi et al., 2004). The THz signal from the InN surface was of the same order of magnitude as that from p-type InAs, one of the strongest semiconductor surface emitters of THz radiation. We have extended these measurements to include wavelength- (800 to 1500 nm) and background carrier-dependent studies of the THz emission from InN thin films. Figure 3a shows the typical time-domain waveforms of the THz emission normalized to pump and probe power from bulk *n*-InN excited with 800 nm and 1500 nm fs pulses. The amplitude spectrum in Fig. 3b corresponds to the temporal waveform using 800 nm in Fig. 3a. The spectrum peaks at ~ 1 THz, with sharp dips due to atmospheric water vapor. A plot of systematic measurements of THz emission from *n*-InN at excitation wavelengths from 800 nm to 1500 nm is displayed in Fig. 3c. Only a weak dependence on pump wavelength is observed, with the signal dropping by less than a factor of 4 over this spectral range.

Further insight into this data can be obtained by modeling using a one-dimensional momentum conservation and relaxation equation

$$\frac{\partial J_n}{\partial t} = e\left(n\frac{eE}{m^*} + \frac{kT}{m^*}\frac{\partial n}{\partial x}\right) - \frac{J_n}{\tau},$$

with a *k*-dependent effective mass m^* to simulate the sub-ps electron current density J_n. The parameters e, n, E, T, and τ are the elementary electric charge, carrier concentration, electric field, carrier temperature, and momentum relaxation time, respectively. Photo-generated and background electron currents are calculated separately due to their different carrier temperatures. Both

the photo-generated and background hole currents are calculated using drift-diffusion equations assuming their temperatures are invariant at room temperature. The emitted THz signal is then calculated as the volume integration of the time derivative of the total current density.

From this model we have determined that the dominant mechanism for THz generation in bulk InN is the current associated with the diffusion of the photo-generated electrons at elevated electron temperature (photo-Dember effect) and the redistribution of the background electrons under drift. As the excitation wavelength increases, the photoexcited electron temperature decreases by a factor of 5, thereby lowering the THz amplitude. However, the photon number increases by a factor of 1.9 as the excitation wavelength increases, enhancing the THz amplitude. The combination of these effects leads to the weak dependence on excitation wavelength observed in Fig. 3. In addition, the measured THz amplitude from *n*-InN is smaller than that from *p*-InAs due to larger screening from the higher mobility electrons as compared to holes. For example, at the fixed bulk carrier concentration of 10^{18} cm^{-3}, the calculations in Fig. 4 show that the THz amplitude from *p*-InN would be more than an order of magnitude larger than from *n*-InN. Moreover, the measured normalized THz amplitude from InN shown in Fig. 4 decreases by about one order of magnitude as the bulk carrier concentration n_{bulk} increases by one order of magnitude. Although there are several other effects which contribute to the THz amplitude, including photo-excited electron temperature, mobility, absorption, and carrier lifetime, screening from carriers appears to be the dominant effect. There is no discernable difference between the In- and N-face InN samples, as expected for the improved crystalline quality and concomitant low background electron density and high mobility for both polarities.

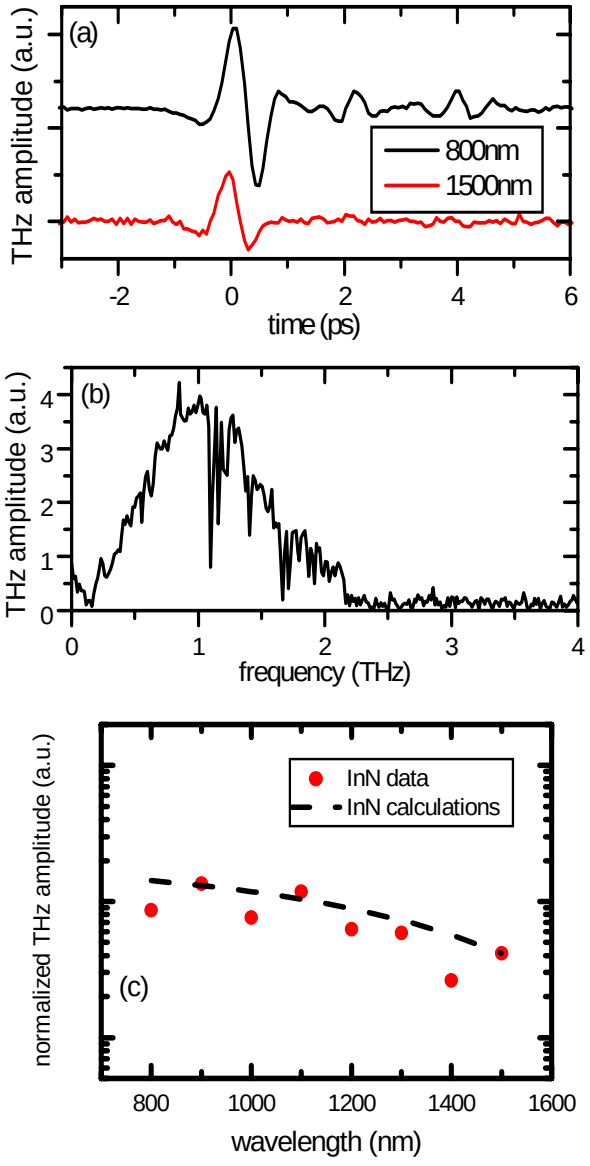

Fig. 3. (a) Time-domain THz signal from InN excited by 800 nm and 1500 nm fs pulses; (b) amplitude spectrum after FFT of the termporal waveform using 800 nm pulses; (c) Pump wavelength dependence of THz amplitude.

4. CONCLUSION

InN and InN/InGaN nanostructures are promising materials for THz sources pumped by low cost 1550 nm fs fiber and CW lasers because of their combination of small bandgap, large saturation velocity and intervalley spacing, and ability to support MV internal electric fields based on spontaneous polarization. Time domain THz

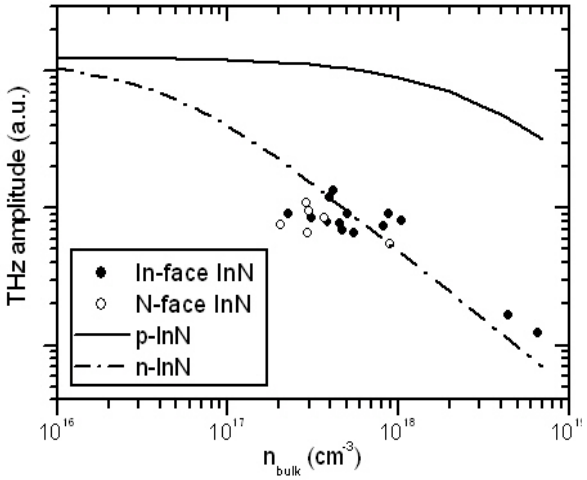

Fig. 4. Background carrier density dependence of THz emission from InN.

spectroscopy shows only a weak dependence of the THz signal on pump wavelength, dropping by less than a factor of 4 in moving from 800 nm to 1500 nm excitation. Modeling shows that the dominant mechanism for THz generation in bulk InN is the current associated with the diffusion of the photo-generated electrons at elevated electron temperature (photo-Dember effect) and the redistribution of the background electrons under drift, with larger screening from the higher mobility electrons as compared to holes. While these studies indicate that InN can approach the performance of the best bulk semiconductor THz emitter, p-InAs, through compensation/p-type doping, manipulation of the large internal electric fields in InN/InGaN nanostructures should enable significant improvements in THz emitters.

REFERENCES

Ascazubi, R., I. Wilke, K. Denniston, H. Lu, and W.J. Schaff, "Terahertz emission by InN", *Appl. Phys. Lett.*, Vol. 84, No. 23, pp. 4810-4812, 2004.

Barber, J., D.E. Hooks, D.J. Funk, R.D. Averitt, A.J. Taylor, and D. Babikov, "Temperature-dependent far—infrared spectra of single crystals of high explosives using terahertz time-domain spectroscopy" *J. Phys. Chem. A*, Vol. 109, No. 15, pp. 3501-3505, 2005.

Bernardini, F., V. Fiorentini and D. Vanderbilt, "Spontaneous polarization and piezoelectric constants of III-V nitrides", *Phys. Rev. B*, Vol. 56, No. 16, pp. R10024-R10027, 1997.

Bjarnason, J.E., T.L.J. Chan, A.W.M. Lee, E.R. Brown, D.C. Driscoll, M. Hanson, A.C. Gossard, and R.E. Muller, "ErAs:GaAs photomixer with two-decade tunability and 12 μ W peak output power", *Appl. Phys. Lett.,* Vol. 85, No. 18, pp. 3983-3985, 2004.

Federici, J.F., B. Schulkin, H. Feng, D. Gary, R. Barat, F. Oliveira, and D. Zimdars, "THz imaging and sensing for security applications-explosives, weapons and drugs", *Semicond. Sci. and Tech.*, Vol. 20, No. 7, pp. S266-S280, 2005.

Gallinat, C.S., G. Koblmüller, J.S. Brown, S. Bernardis, J.S. Speck, G.D. Chern, E.D. Readinger, H. Shen, and M. Wraback, "In-polar InN grown by plasma-assisted molecular beam epitaxy", *Appl. Phys. Lett.,* Vol. 89, No. 3, Art. 032109, 2006.

Globus, T. R., D. L. Woolard, T. Khromova, T. W. Crowe, M. Bykhovskaia, B. L. Gelmont, J. Hesler, and A. C.Samuels**,** "THz-spectroscopy of biological molecules", *J. Biologic. Phys.*, Vol. 29, Nos. 2-3, pp. 89-100, 2003.

Koblmüller, G., C.S. Gallinat, S. Bernardis, J.S. Speck, G.D. Chern, E.D. Readinger, H. Shen, and M. Wraback, "Optimization of the surface and structural quality of N-face InN grown by molecular beam epitaxy", *Appl. Phys. Lett.*, Vol. 89, No. 7, Art. 71902, 2006.

Liang, W., K.T. Tsen, D.K. Ferry, H. Lu, and W.J. Schaff, "Field-induced nonequilibrium electron distribution and electron transport in a high-quality inn thin film grown on GaN", *Appl. Phys. Lett.*, Vol. 84, No. 18, pp. 3681-3683, 2004.

Liu, H., Liu, Y. Chen, T. Yuan, F. Al-Douseri, J. Xu, and X.-C. Zhang, "Quantitative analysis of ammonia by THz time-domain spectroscopy", SPIE Proc. Vol. 5268, pp.43-52, 2004.

Liu, K., J. Xu, T. Yuan, and X-.C. Zhang, Phys. Rev. **B73**, 155330 (2006).

Markelz, A.G., A. Roitberg, and E.J. Heilweil, "Pulsed terahertz spectroscopy of DNA, bovine serum albumin and collagen between 0.1 and 2.0 THz", *Chem. Phys. Lett.*, Vol. 320, Nos. 1-2, pp. 42-48, 2000.

Samuels, A.C., J.O. Jensen, R.D. Suenram, A.H. Walker, and D.L. Woolard, "Microwave spectroscopy of chemical warfare agents: prospects for remote sensing", *SPIE Proc.*, Vol. 3703, pp. 121-129, 1999.

Shen, Y.C., T. Lo, P.F. Taday, B.E. Cole, W.R. Tribe, and M.C. Kemp, "Detection and identification of explosives using terahertz pulsed spectroscopic imaging", *Appl. Phys. Lett.*, Vol. 86, No. 24, Art. 241116, 2005.

Turchinovich, D., P. Uhd Jepsen, B.S. Monozon, M. Koch, S. Lahmann, U. Rossow, and A. Hangleiter, "Ultrafast polarization dynamics in biased quantum wells under strong femtosecond optical excitation", *Phys. Rev. B*, Vol. 68, No.24, Art. 241307(R), 2003.

Woolard, D.L., T. R. Globus, B. L. Gelmont, M. Bykhovskaia, A. C. Samuels, D. Cookmeyer, J. L. Hesler, T. W. Crowe, J. O. Jensen, J. L. Jensen and W.R. Loerop, "Submillimeter-wave phonon modes in DNA macromolecules", *Phys. Rev E.*, Vol. 65, No.5, Art. 051903, 2002.

Wu, J., W. Walukiewicz, K. M. Yu, J. W. Ager III, E. E. Haller, H. Lu, W. J. Schaff, Y. Saito, and Y. Nanishi, "Unusual properties of the fundamental bandgap of InN", *Appl. Phys. Lett.*, Vol. 80, No. 21, pp. 3967-3969, 2002.

Xu, K. and A. Yoshikawa, "Effects of film polarities on InN growth by molecular-beam epitaxy", *Appl. Phys. Lett.*, Vol. 83, No. 2, pp. 251-253, 2003.

Zhang, X.-C., B. B. Hu, J. T. Darrow and D. H. Auston, "Generation of femtosecond electromagnetic pulses from semiconductor surfaces", *Appl. Phys Lett.*, Vol. 56, No. 11, pp. 1011-1013, 1990.

Indium Nitride: A New Material for High Efficiency, Compact, 1550 nm Laser-Based Terahertz Sources in Explosives Detection and Concealed Weapons Imaging

M. Wraback, G. Chern, E. Readinger, and H. Shen,
U.S. Army Research Laboratory

G. Koblmueller, C. Gallinat, and J. Speck
University of California, Santa Barbara

W. Schaff
Cornell University

What is terahertz?

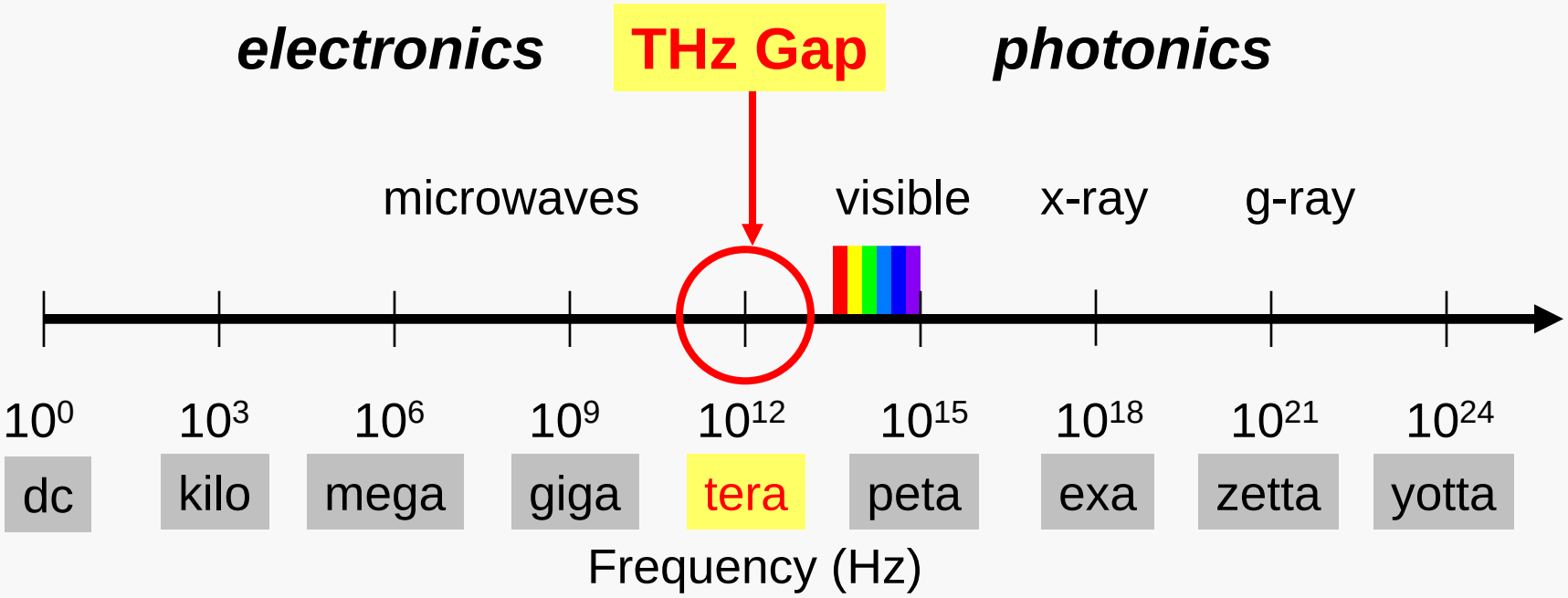

1 THz ~ 1 ps ~ 300 μm ~ 33 cm^{-1} ~ 4.1 meV ~ 47.6 ºK

THz Applications - Explosives

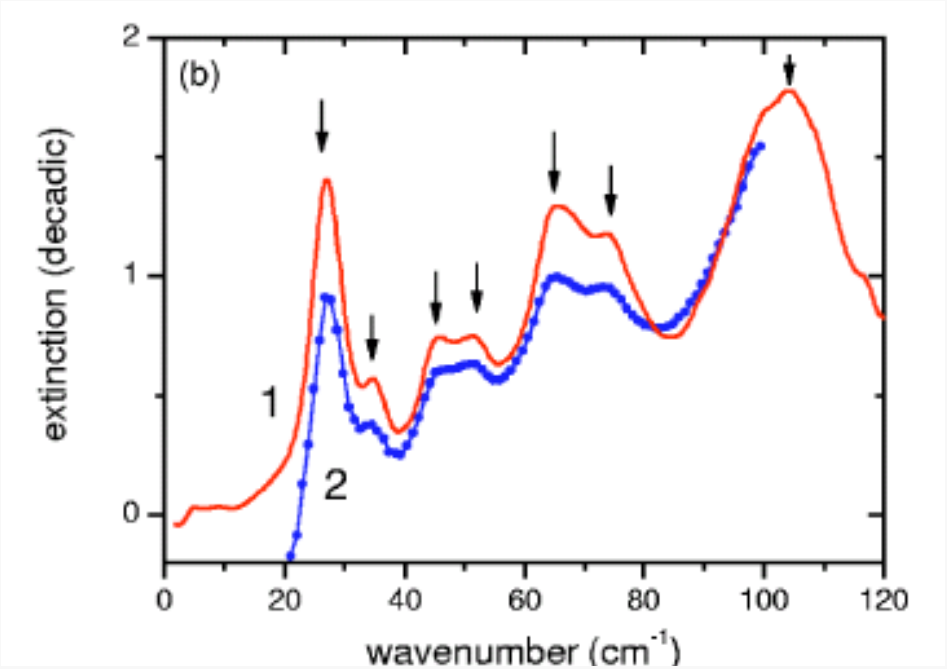

THz spectra of RDX using pulsed spectrometer (1) compared to FTIR(2) Y.C. Shen et. al. APL (2005)

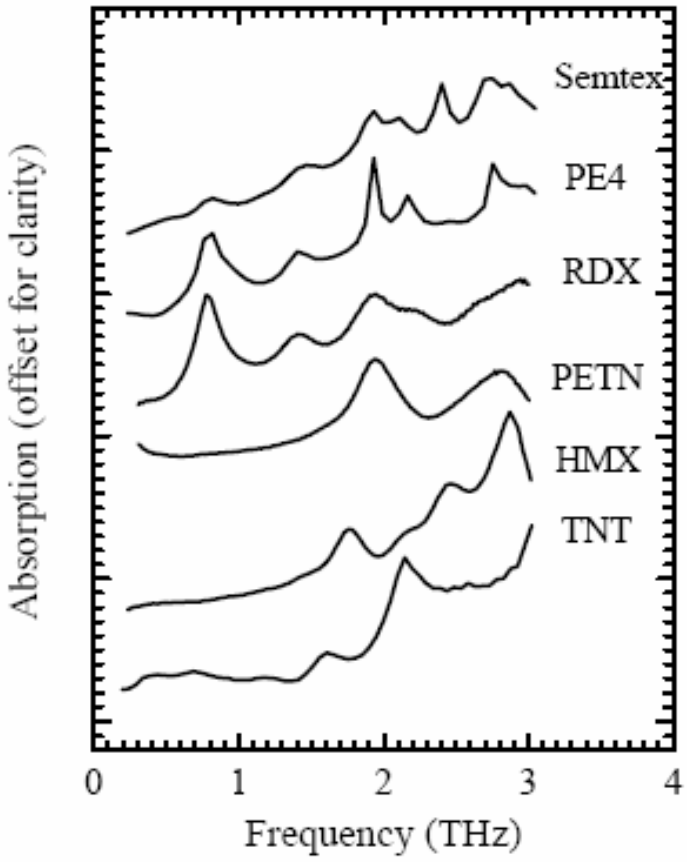

Time-domain THz spectra of various explosives M.C. Kemp, Proc. SPIE 6402, 64020D (2006)

THz Applications - 2

IC chip

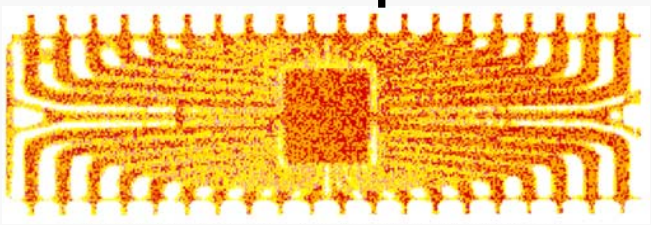

Opt. Lett. 20, 1716 (1995)

Bacon

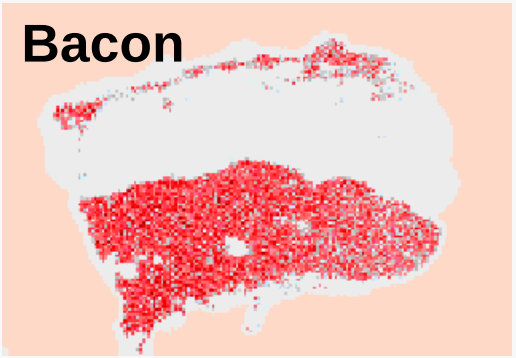

http://www.rpi.edu/~zhangxc

Imaging for Package Inspection and seeing through clothes

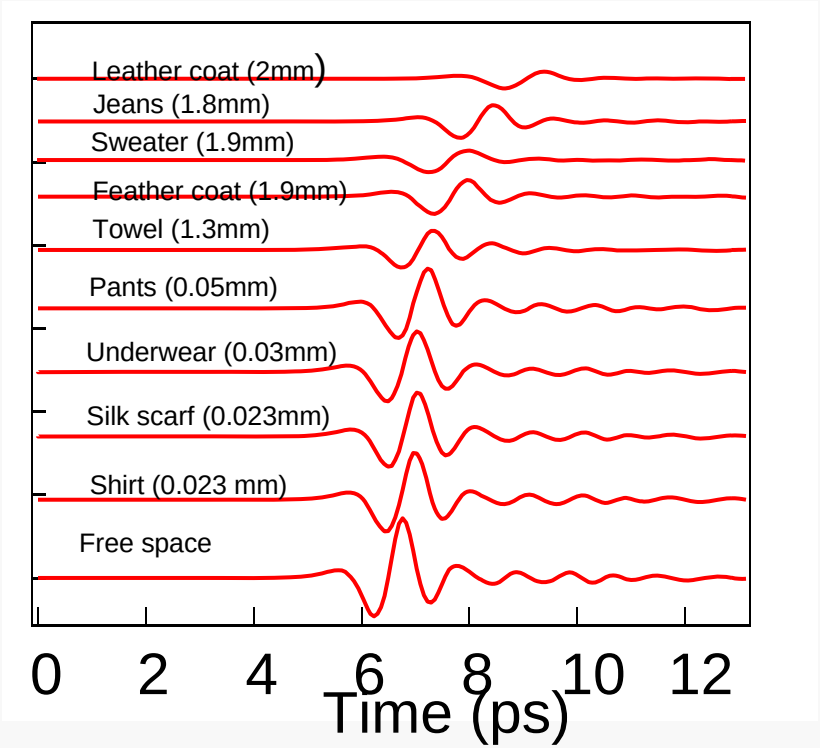

Concealed weapon

Science Vol. 297, 2 Aug. 2002.

Optically Pumped THz Generation

Time-Domain: fs pulses

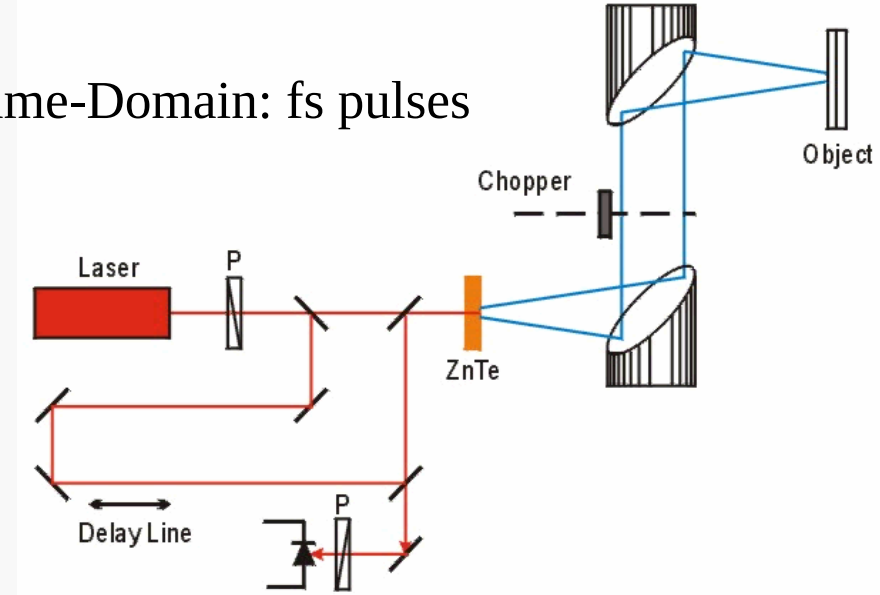

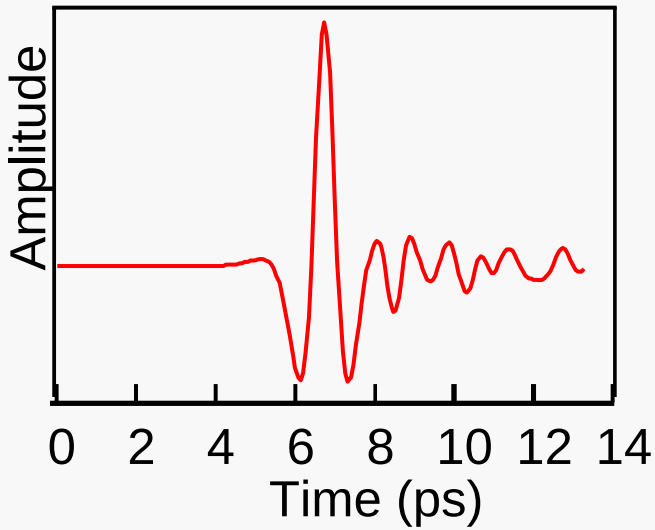

CW: Photomixers

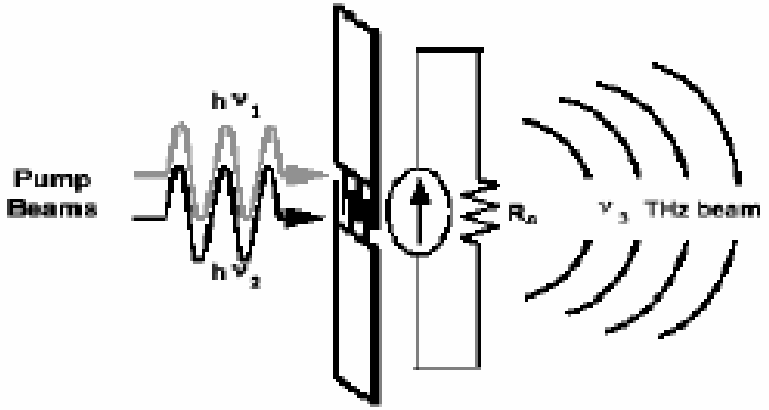

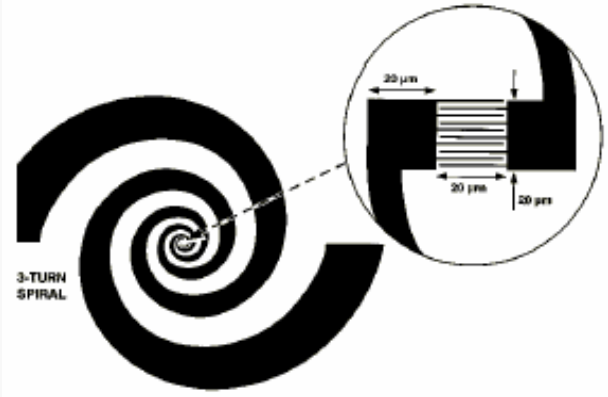

E.R. Brown et al., RSI (2004)

Table-Top Femtosecond Lasers

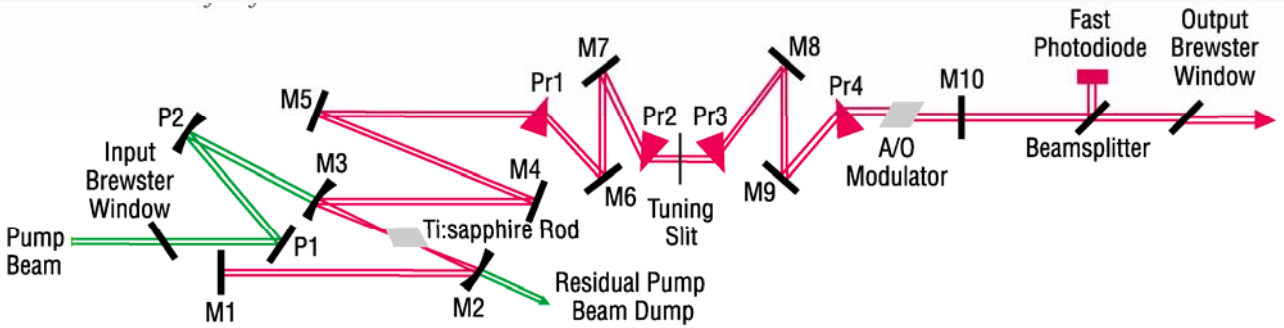

- Size: ~0.8 x 0.3 x 0.2 meters
- Weight: ~30 kg
- Requires optical table
- Price: $100k
- Wavelength: 800 nm

Not suitable for field deployment

Fiber Lasers for THz Generation

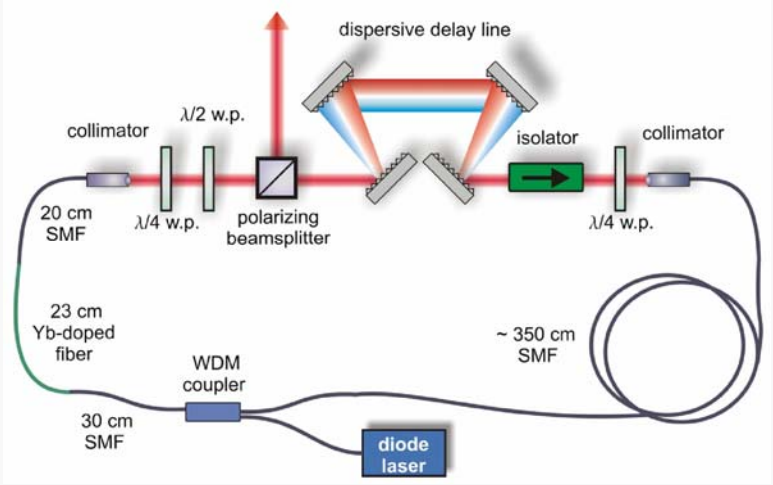

Ilday et al. *Opt. Exp.* **11**(26) 3550 (2003)

- Fiber could enable remote delivery and detection of THz radiation:
  - Sensing in hazardous or difficult to reach places
  - Enhanced mobility of THz probe
- Smaller, lighter, cheaper, more robust than tabletop laser systems
- CW telecom lasers available
- Photomixer efficiency increases as λ^2 (~ 4 x at 1550 nm)

- Problem: Existing THz systems work primarily at 800 nm.

- Question: Can a material be found that would enable one to move to longer wavelengths (1050, 1550 nm) suitable for fiber/telecom lasers while improving overall system efficiency?

III-Nitride Semiconductors

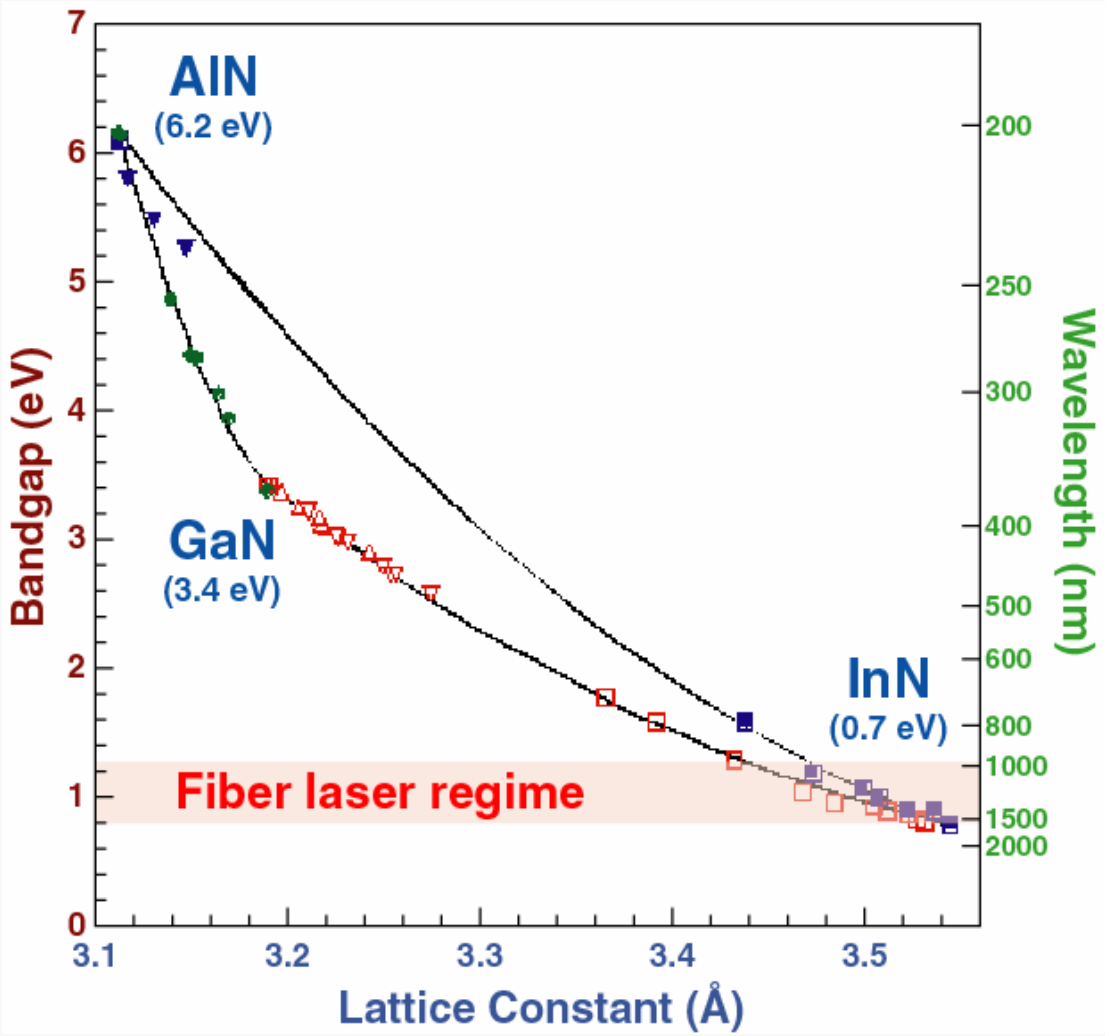

Discovery of the true bandgap of InN below 0.7 eV instead of ~ 2 eV has led to the possibility of devices in the fiber/telecom laser spectral region.

Why InN?

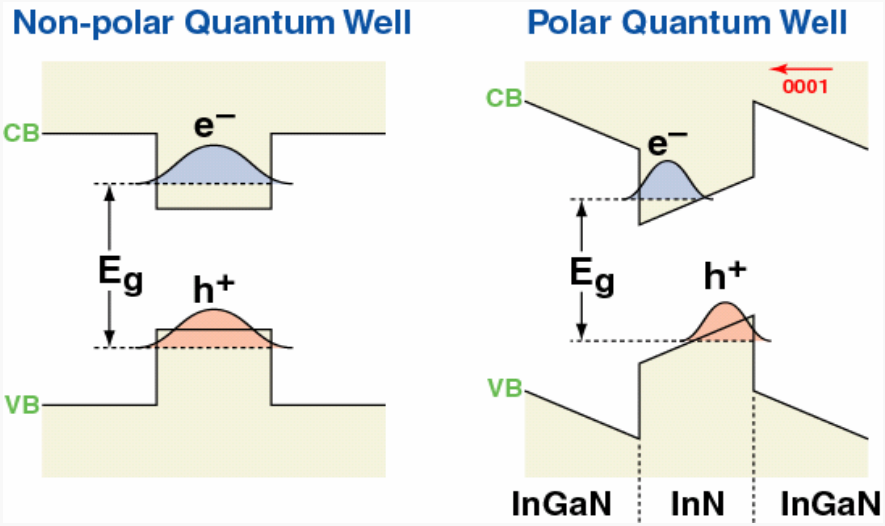

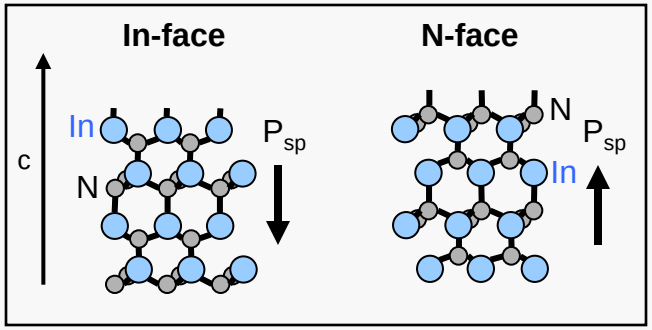

- THz amplitude from <111> antimonide MQWs is ~ 9 times larger than from <100> MQWs (Zhang et al., APL (1990)
- Because of their much larger polarization, InN quantum wells can support a field **more than one order of magnitude larger** than arsenide or antimonide quantum wells (up to 3 MV/cm)
- Higher saturation velocity, larger intervalley spacing, and higher breakdown predicted for InN will lead to higher efficiency photomixers

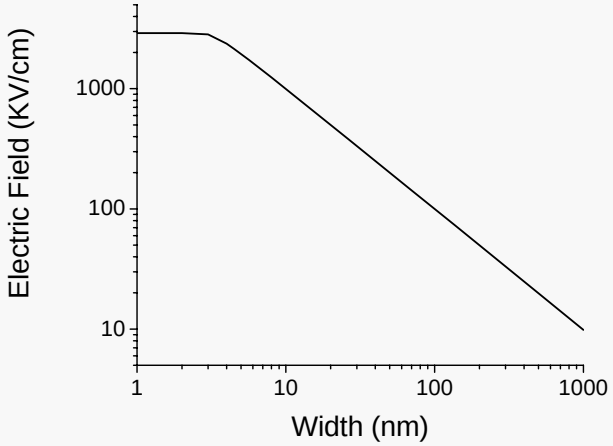

Initial InN Growth and Characterization

ARL E038 ~ 0.87 μm InN/GaN template

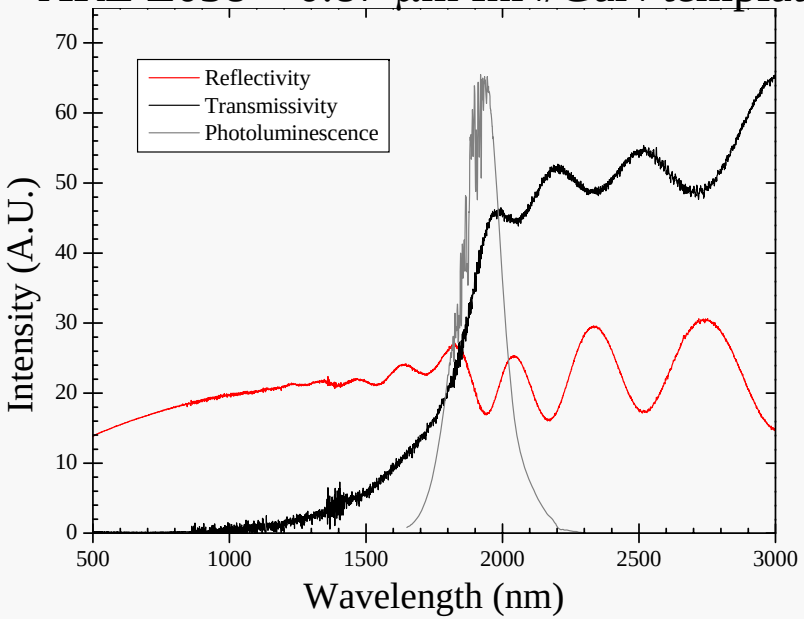

Carrier Conc.: 3.92E+18
Mobility ($cm^2/V*sec$): 924

GS2050 (Cornell) ~7 μm InN/ GaN buffer

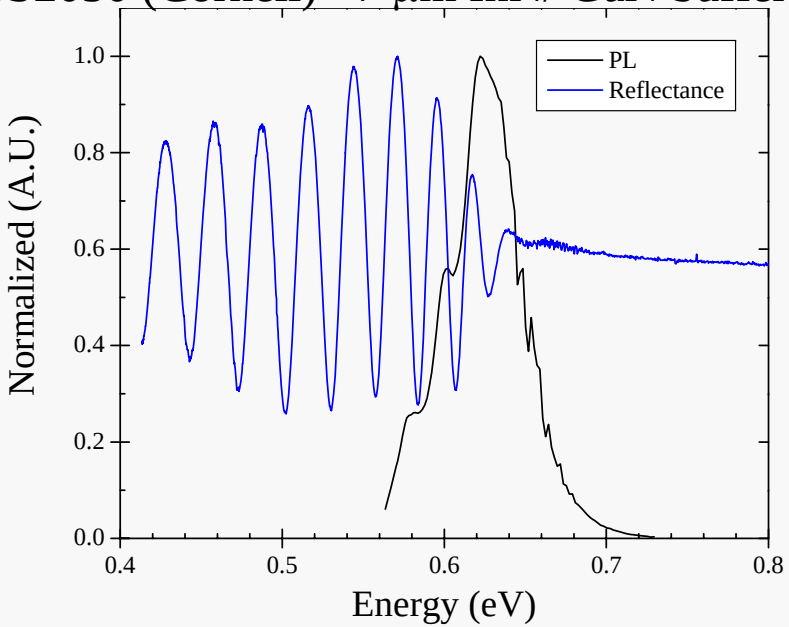

Carrier Conc.: 5.7E+17
Mobility ($cm^2/V*sec$): 1600

- Defect reduction leads to lower autodoping
- Can be achieved through growth of thick InN (defect annihilation) or through thinner InN layers on low defect density templates

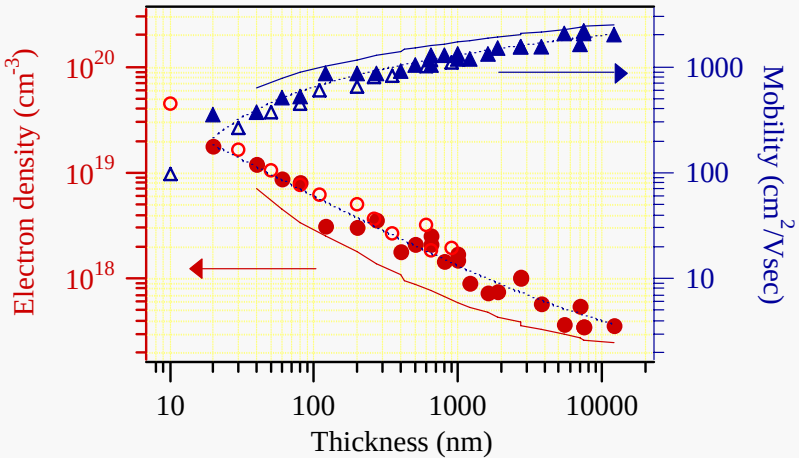

Improved In-face and N-face InN with UCSB

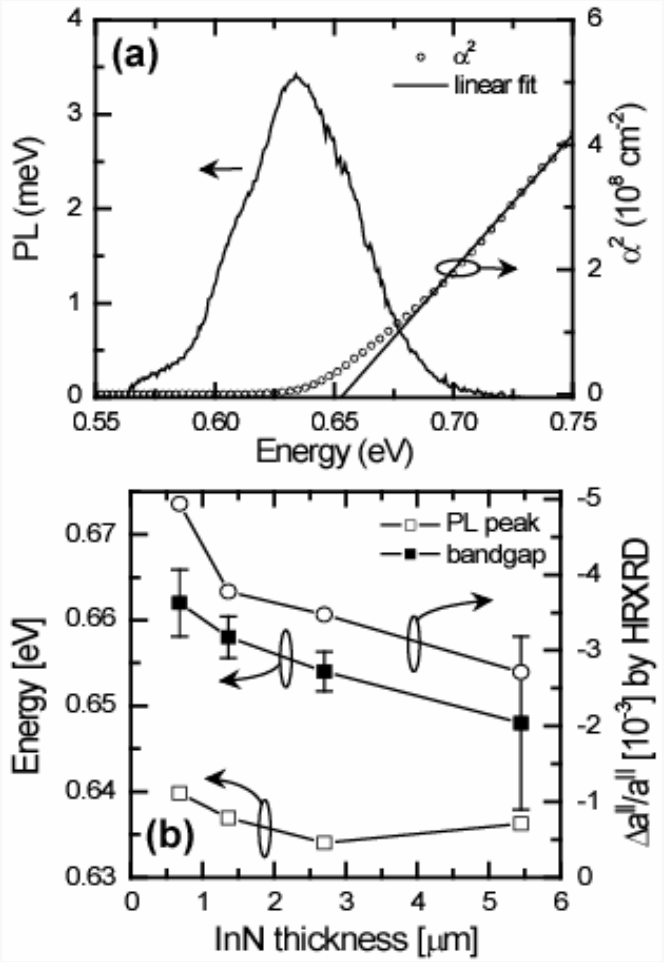

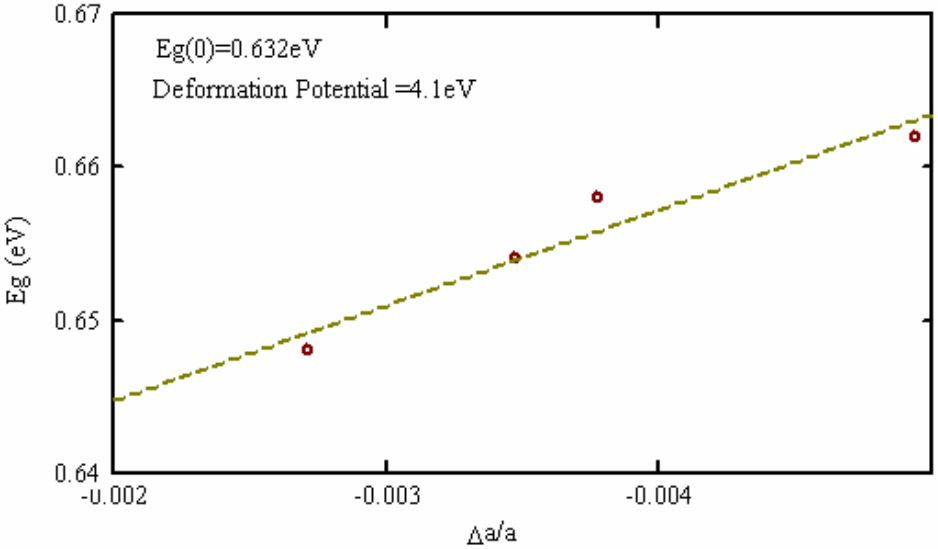

- Unstrained bandgap estimated at ~ 0.63 eV
- PL emission redshifted by 15 to 20 meV

Electron accumulation layer in InN

- Fermi-level pinning above E_c
  - band bending
  - electron accumulation from donor-type surface states

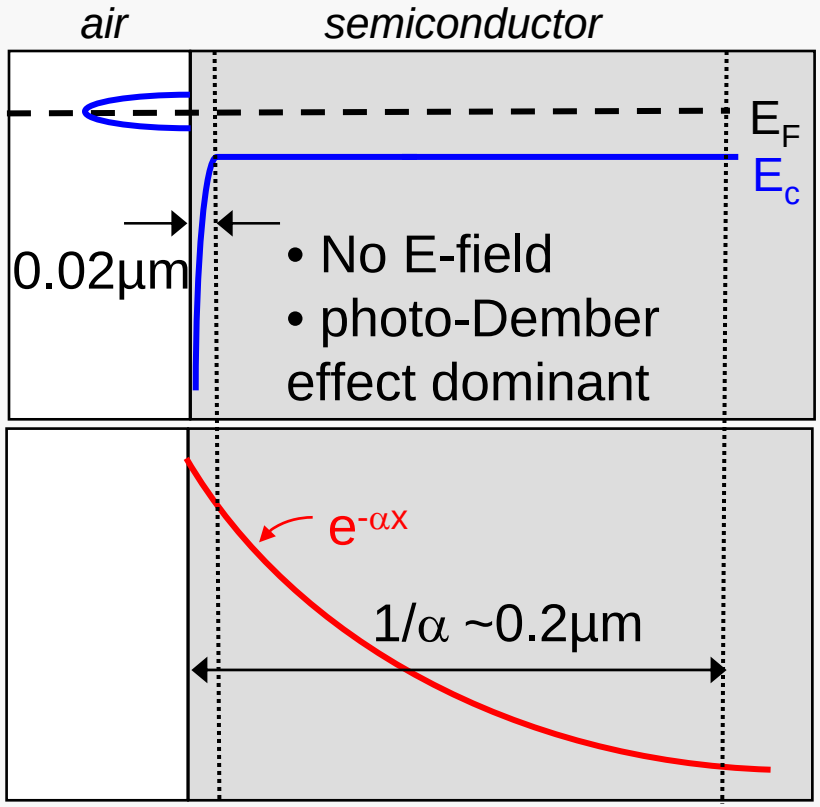

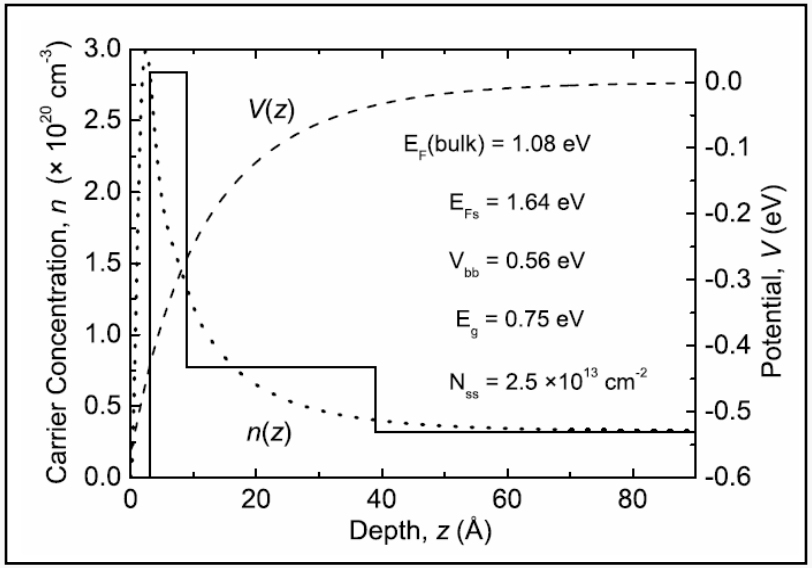

I. Mahboob, T. D. Veal, C. F. McConville, H. Lu, and W. J. Schaff, "Intrinsic electron accumulation at clean InN surfaces," *Phys. Rev. Lett.* **92**, 036804-1 (2004).

Accumulation Layer and Bulk Electron Densities

$$n_{bulk} = (\sigma_{sheet} - \sigma_{surface})/d$$

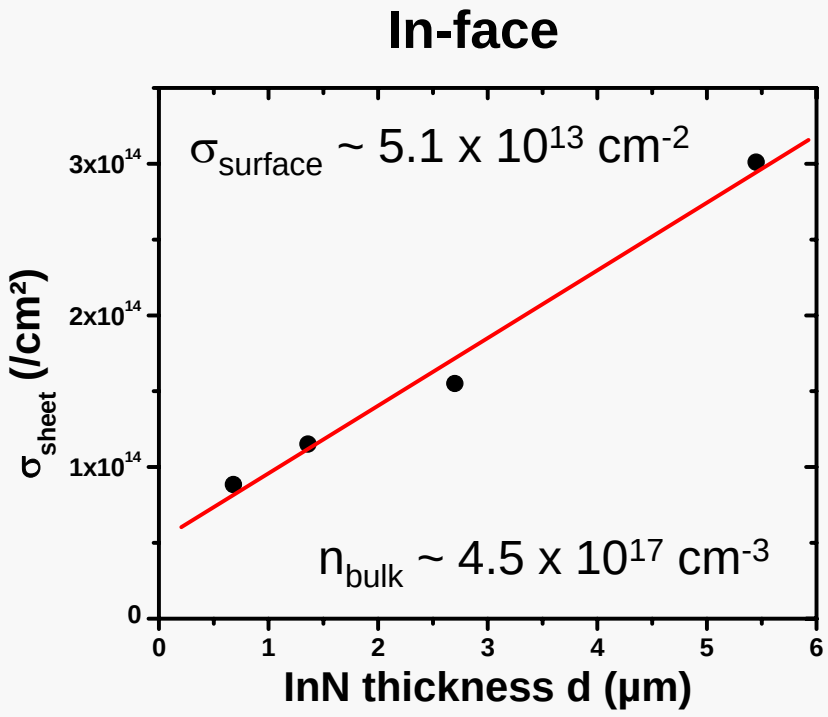

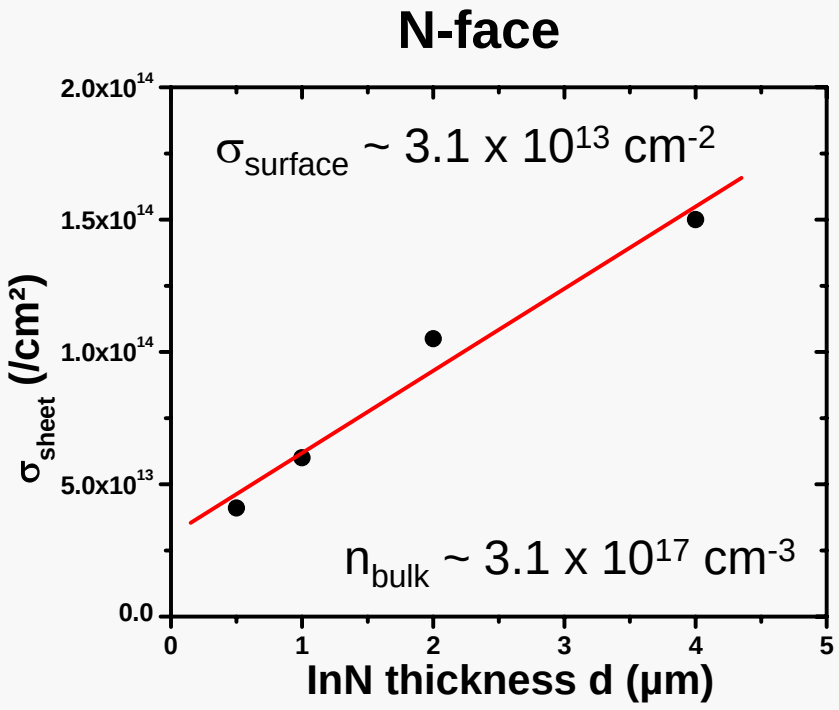

Experimental setup – 800 nm

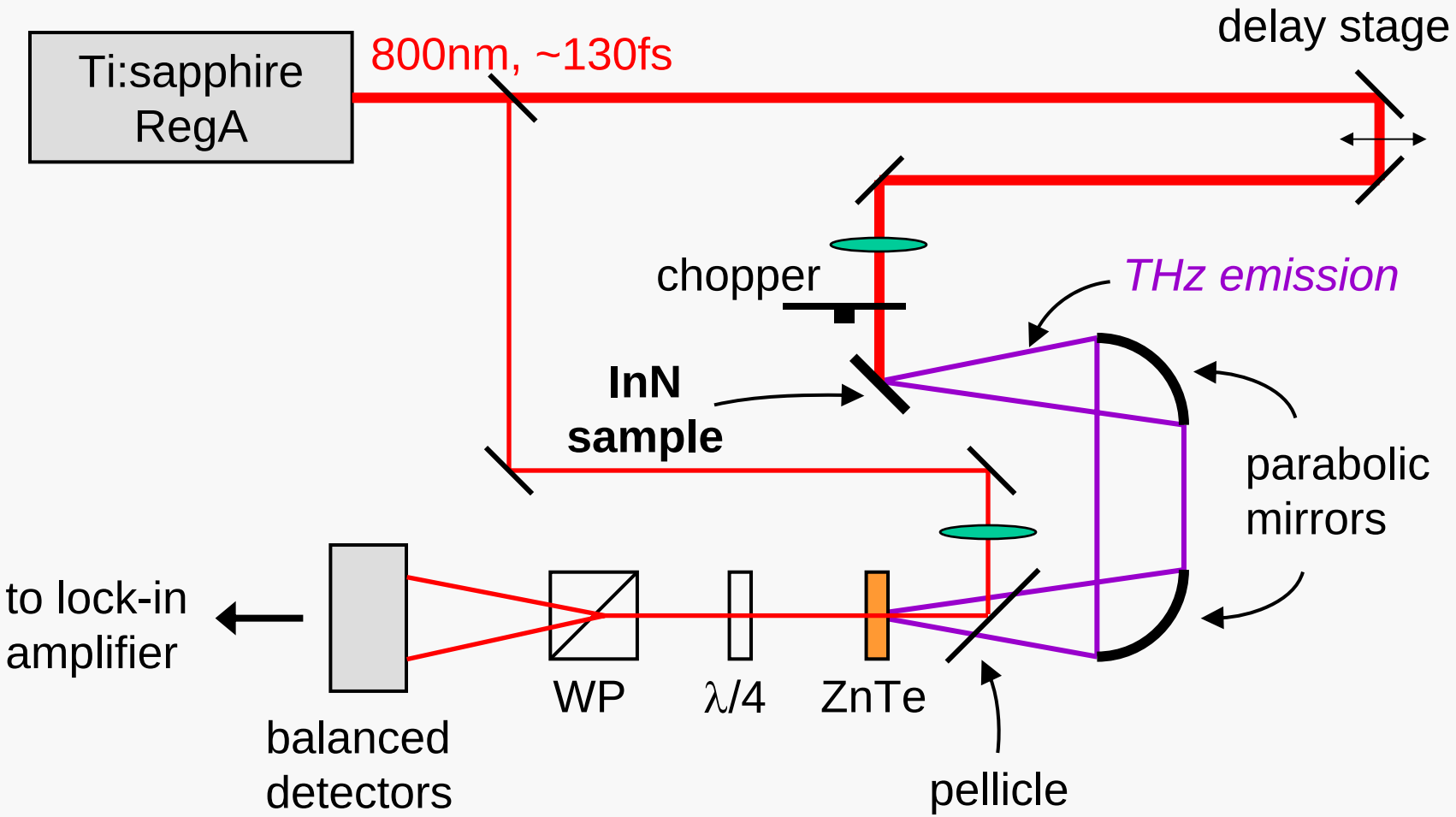

Experimental setup - tunable

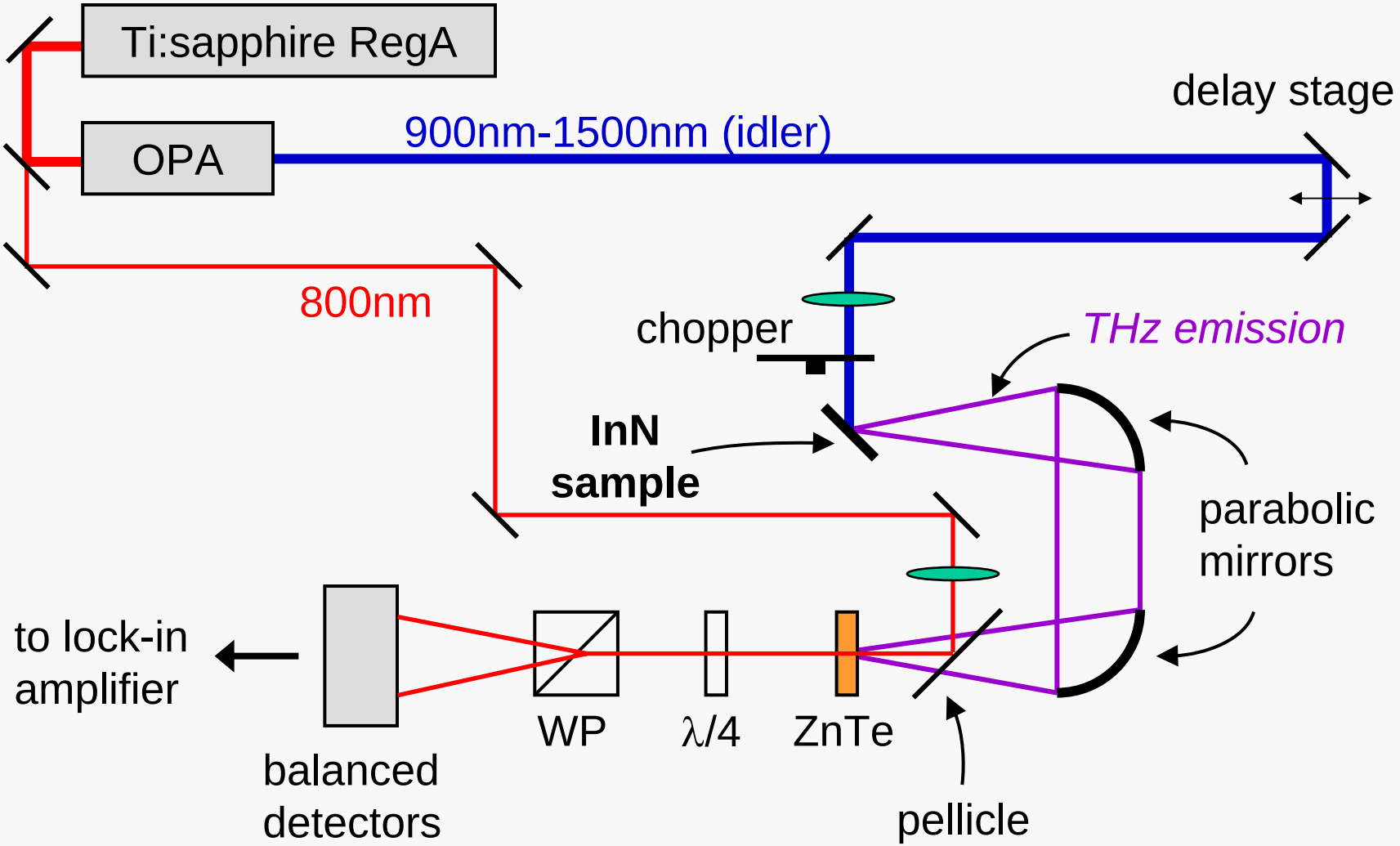

Terahertz emission from InN

Time-resolved pulse

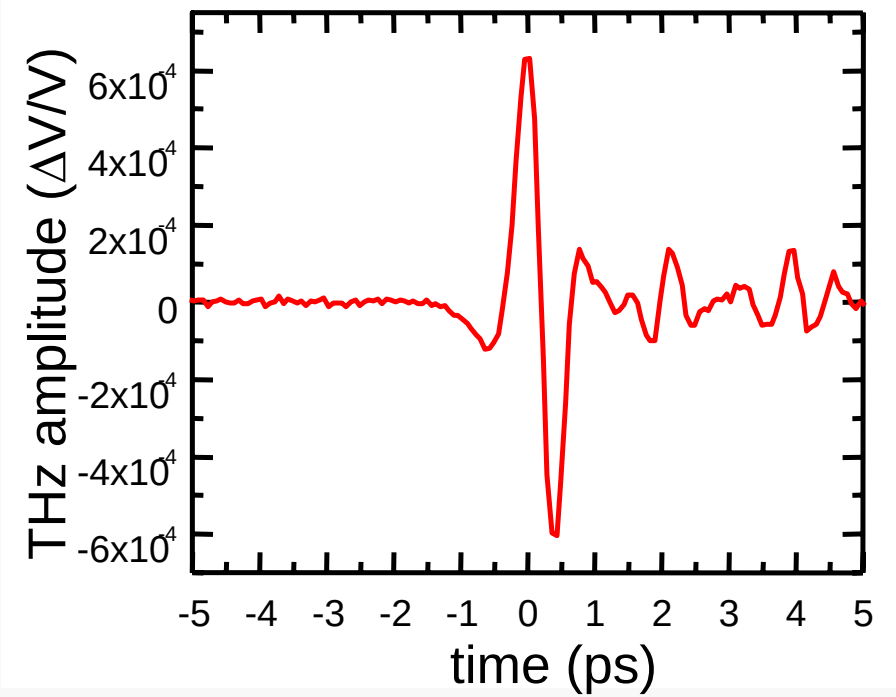

Fourier transform of time-resolved pulse

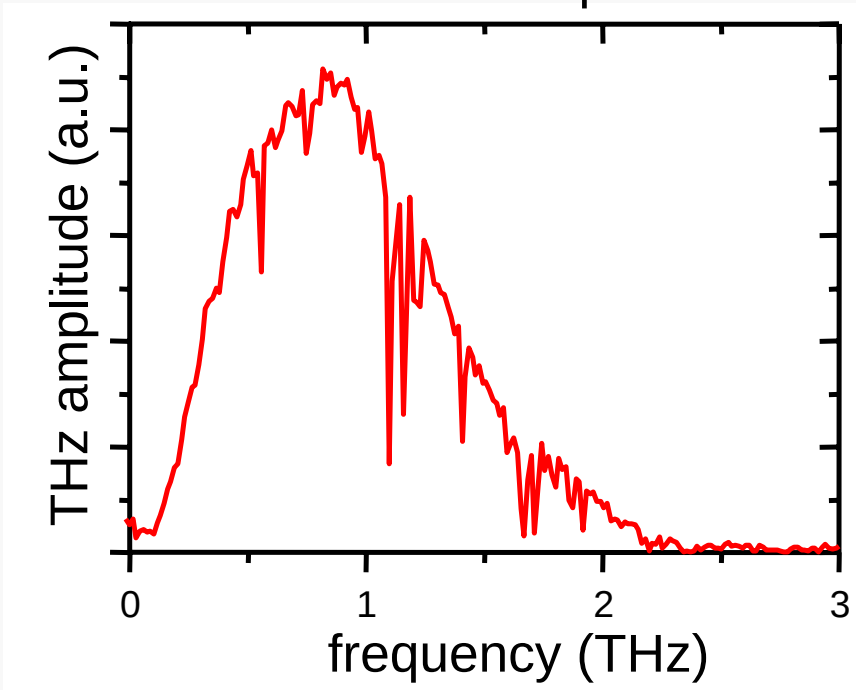

* spectral dips due to H_2O absorption

Wavelength dependence

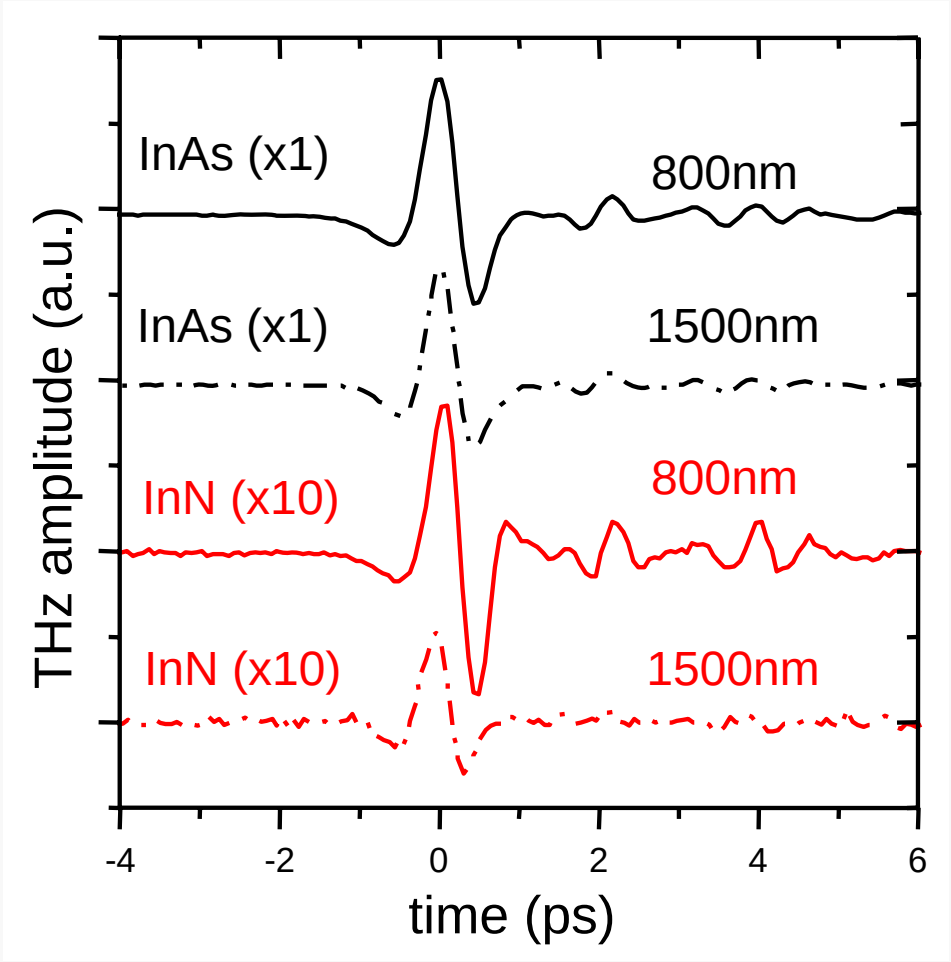

- InN ~10x smaller than InAs
  - InAs is *p*-type (compared to *n*-InN)
  - InAs has low doping (~10^{16} cm^{-3} compared to ~10^{17} cm^{-3} for InN)
- THz amplitude for 800 nm and 1500 nm cases comparable

Wavelength dependence

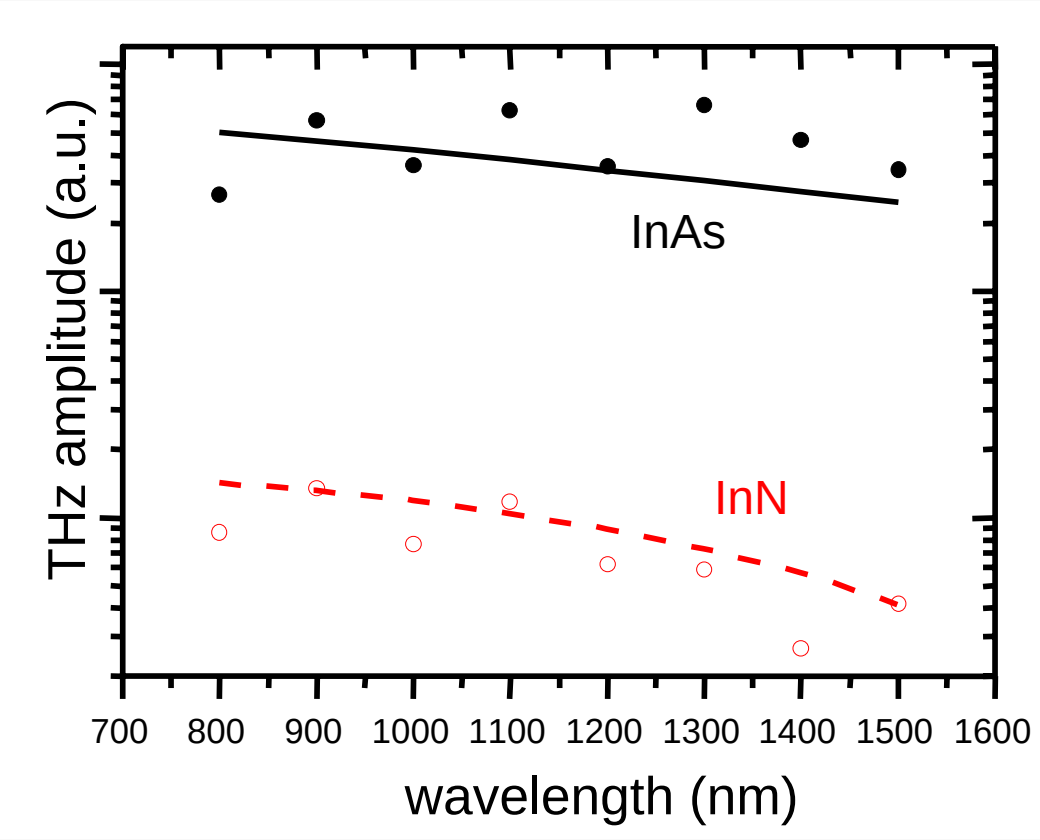

- THz amplitude decreases with diminishing photo-excited electron temperature (as λ increases)
- But THz amplitude increases with increasing photon number (as λ increases)
- InAs (E_g=0.36eV) – overall decrease by <2
- InN (E_g=0.66eV) – overall decrease by <4

Bulk carrier concentration and mobility dependence

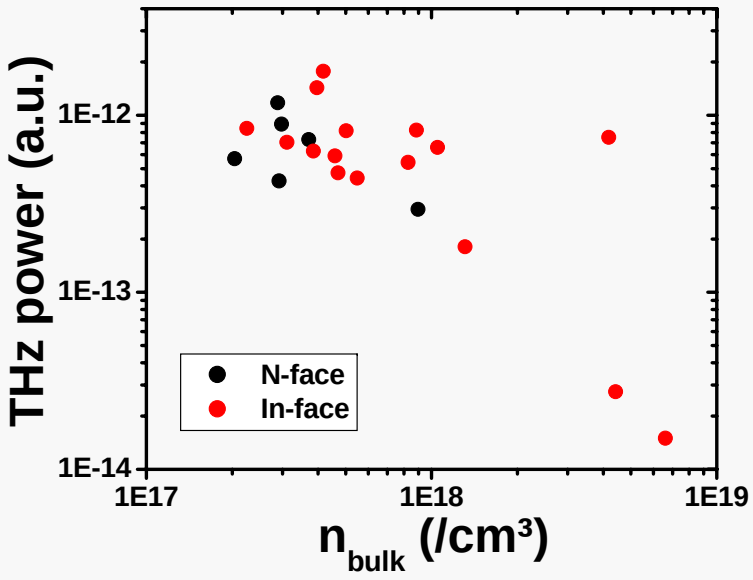

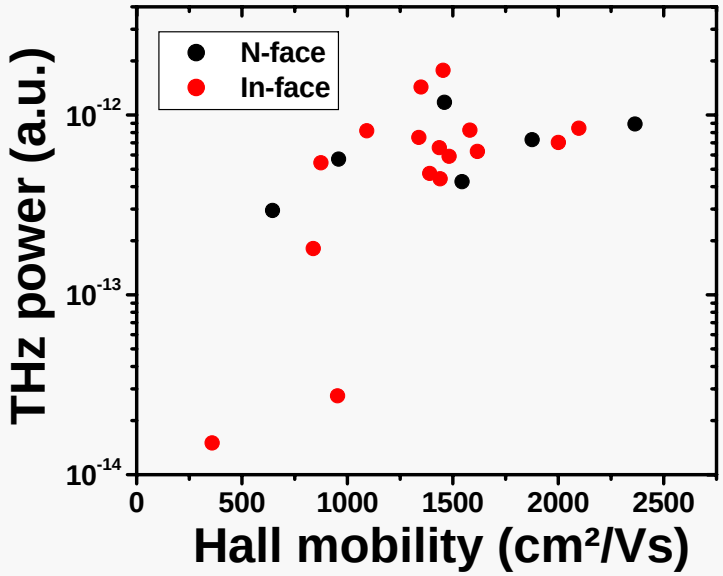

- N-face and In-face InN have similar dependence on n_{bulk}
- THz power decreases as n_{bulk} increases
- Difficult to grown low n_{bulk} ($< 10^{17}$ cm^{-3}) InN films

- N-face and In-face polarities show similar dependence on mobility
- THz amplitude increases with mobility

Terahertz generation mechanism

- photo-Dember effect - difference between carrier mobilities
- screening due to background or bulk carriers n_{bulk}

$$J_{net} = J_{diffusion} + J_{bulk}$$

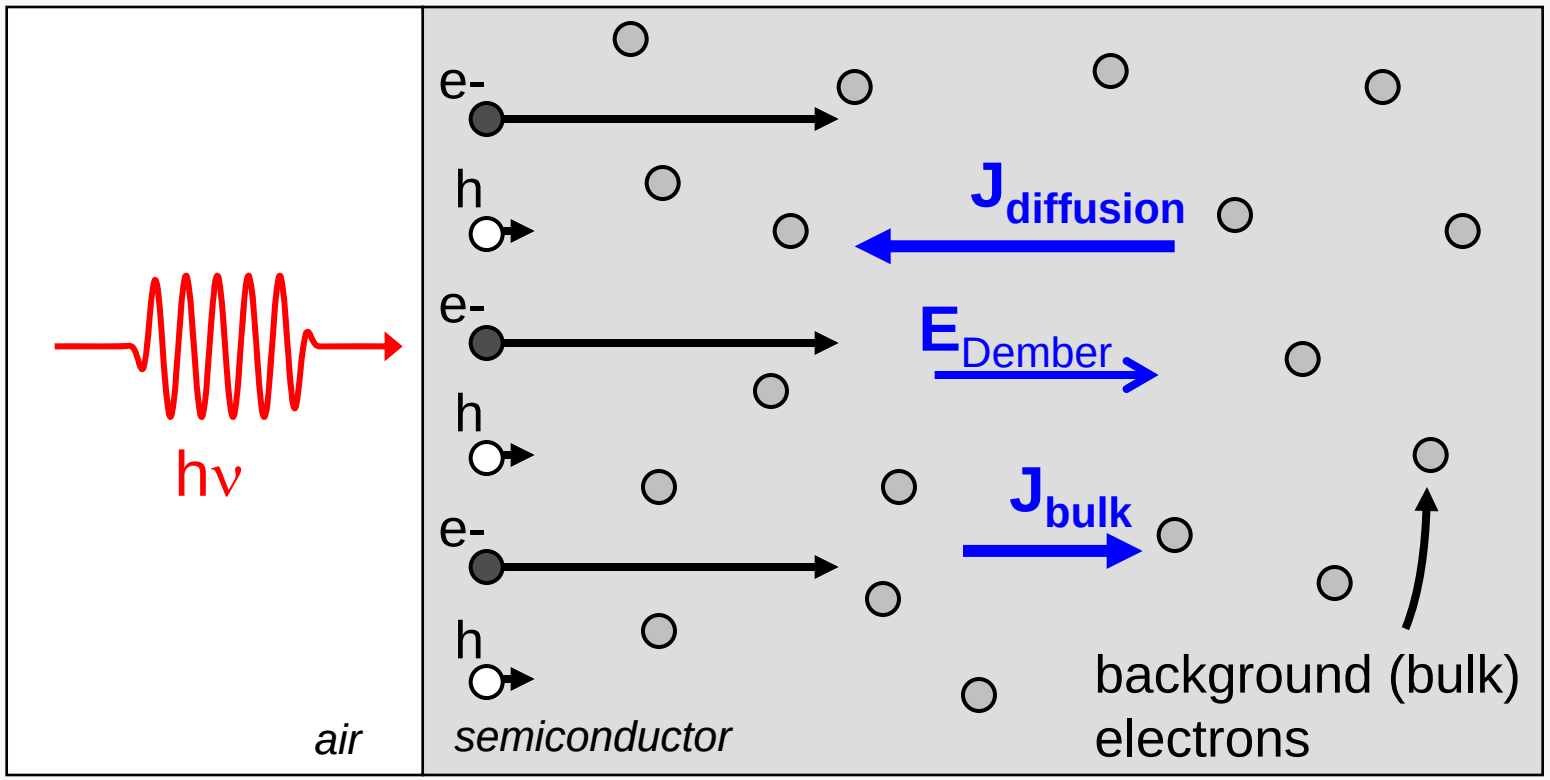

Calculations

$$\frac{\partial J_n}{\partial t} = e\left(n\frac{eE}{m^*} + \frac{kT}{m^*}\frac{\partial n}{\partial x} \right) - \frac{J_n}{\tau}$$

- k dependent effective mass

- Photo-generated and background electron currents calculated separately due to their different carrier temperatures

- Both the photo-generated and background hole currents calculated using drift-diffusion equations assuming their temperatures were invariant at room temperature

- The emitted THz signal calculated as the volume integration of the time derivative of the total current density.

Discussion

• The dominant currents are the diffusion of the photo-generated electrons at elevated electron temperature and the redistribution of the background electrons under drift

• Wavelength Dependence: wavelength increases, photon number increases, electron temperature decreases, more for InN than InAs

• THz amplitude from n-InN is about an order of magnitude smaller than from p-InAs due to larger screening from the higher mobility electrons as compared to holes, as well as the higher background electron density.

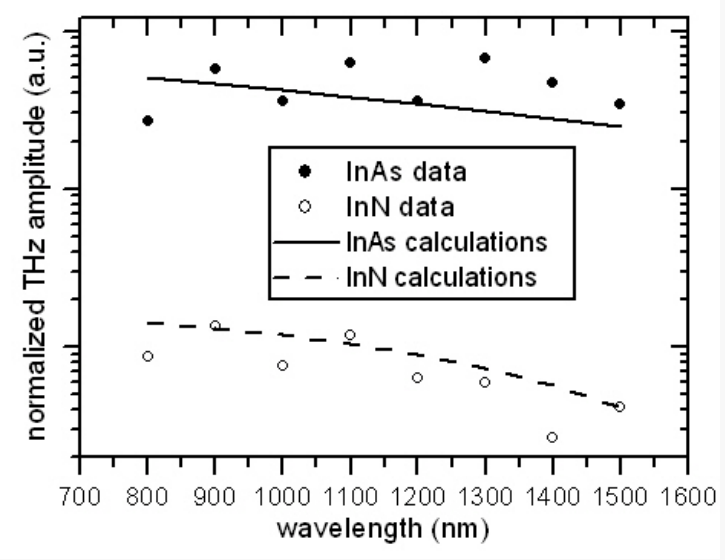

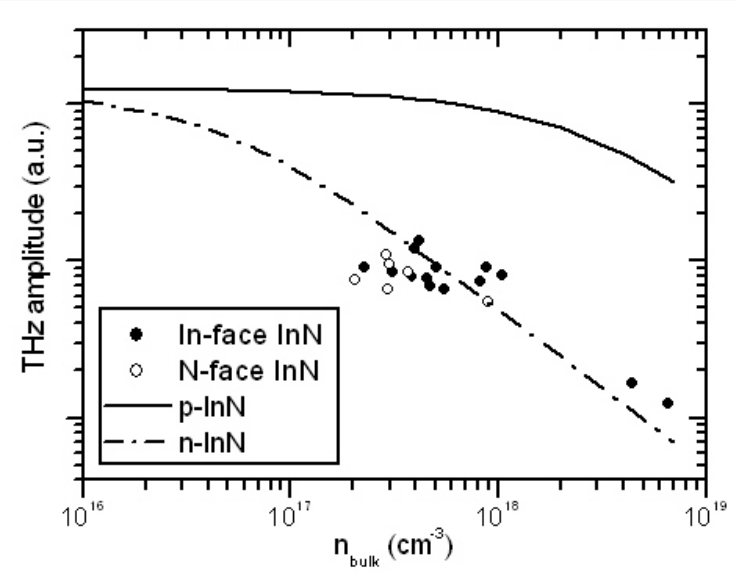

InN/InGaN Quantum wells

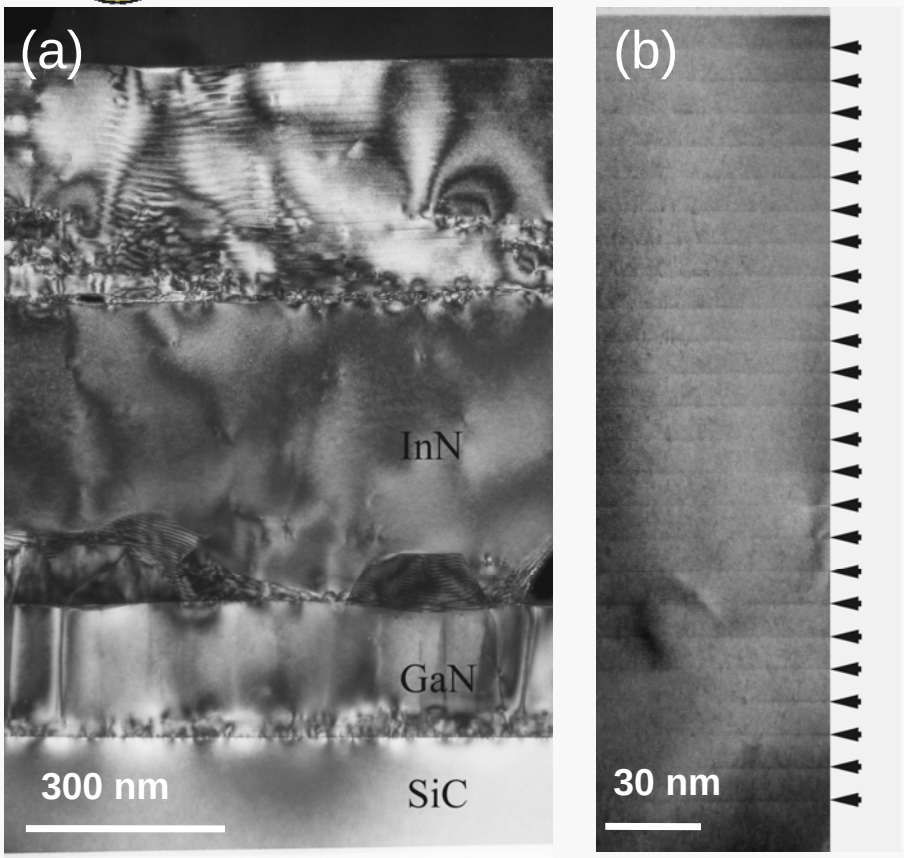

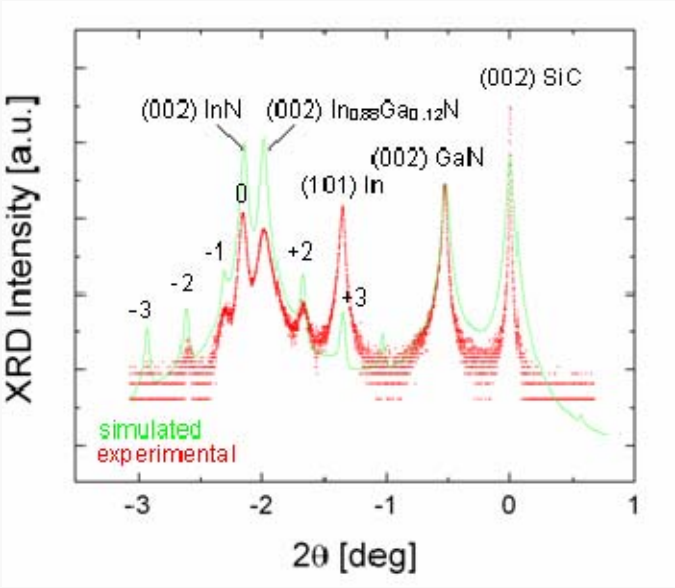

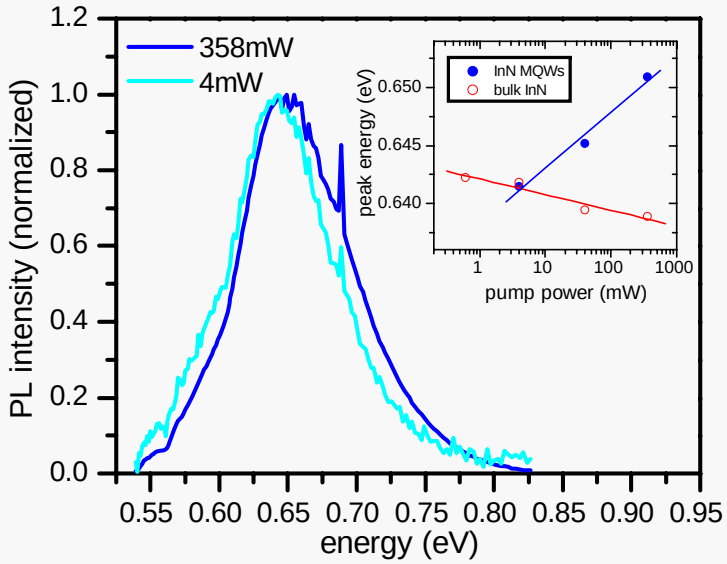

- **Cross–sectional TEM images of $InN/In_{0.88}Ga_{0.12}N$ MQWs on InN/GaN/SiC**
- **Clear and uniform interfaces between InN wells (1.5 nm) and InGaN barriers (15 nm)**

Comparison of THz from InN/InGaN MQW and bulk InN

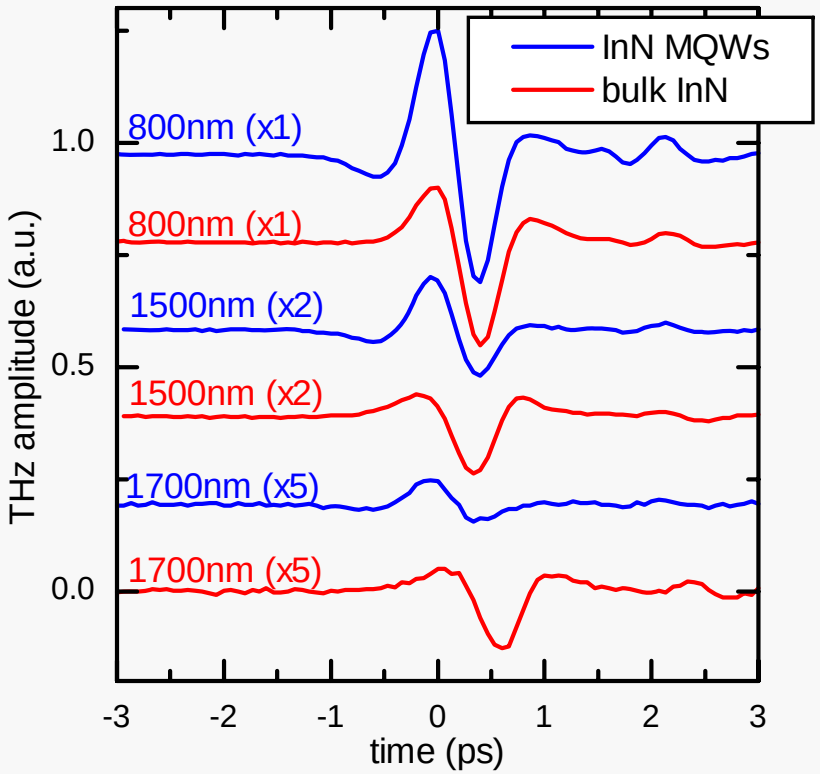

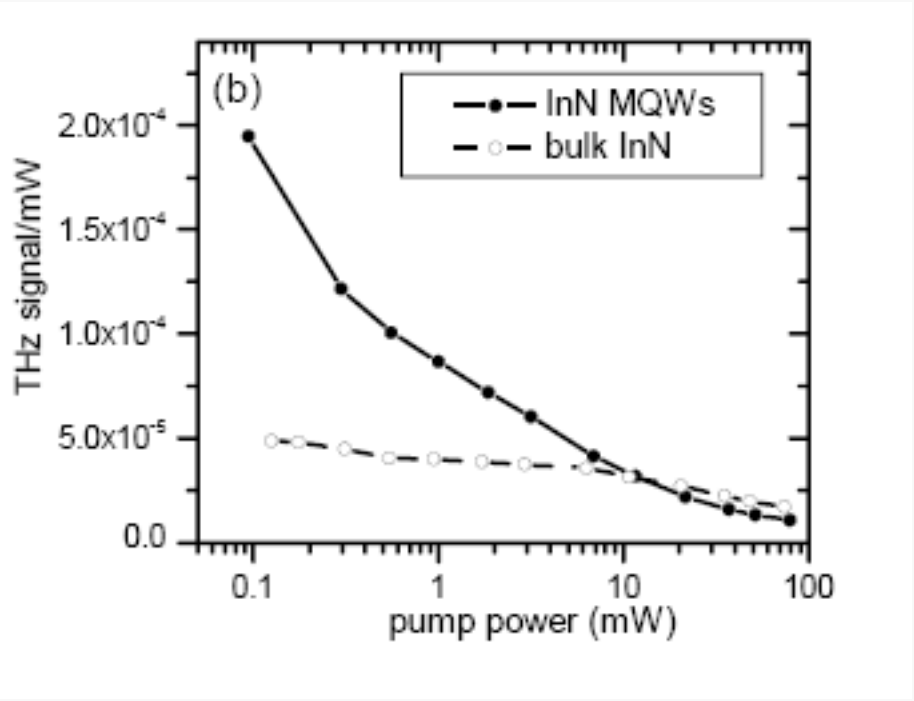

- **MQW THz signal is larger than bulk InN signal for 800 nm pumping, but decreases more with increasing wavelength**
- **MQW THz signal increases relative to bulk InN signal for decreasing 800 nm pump power**

THz from InN/InGaN MQW Model

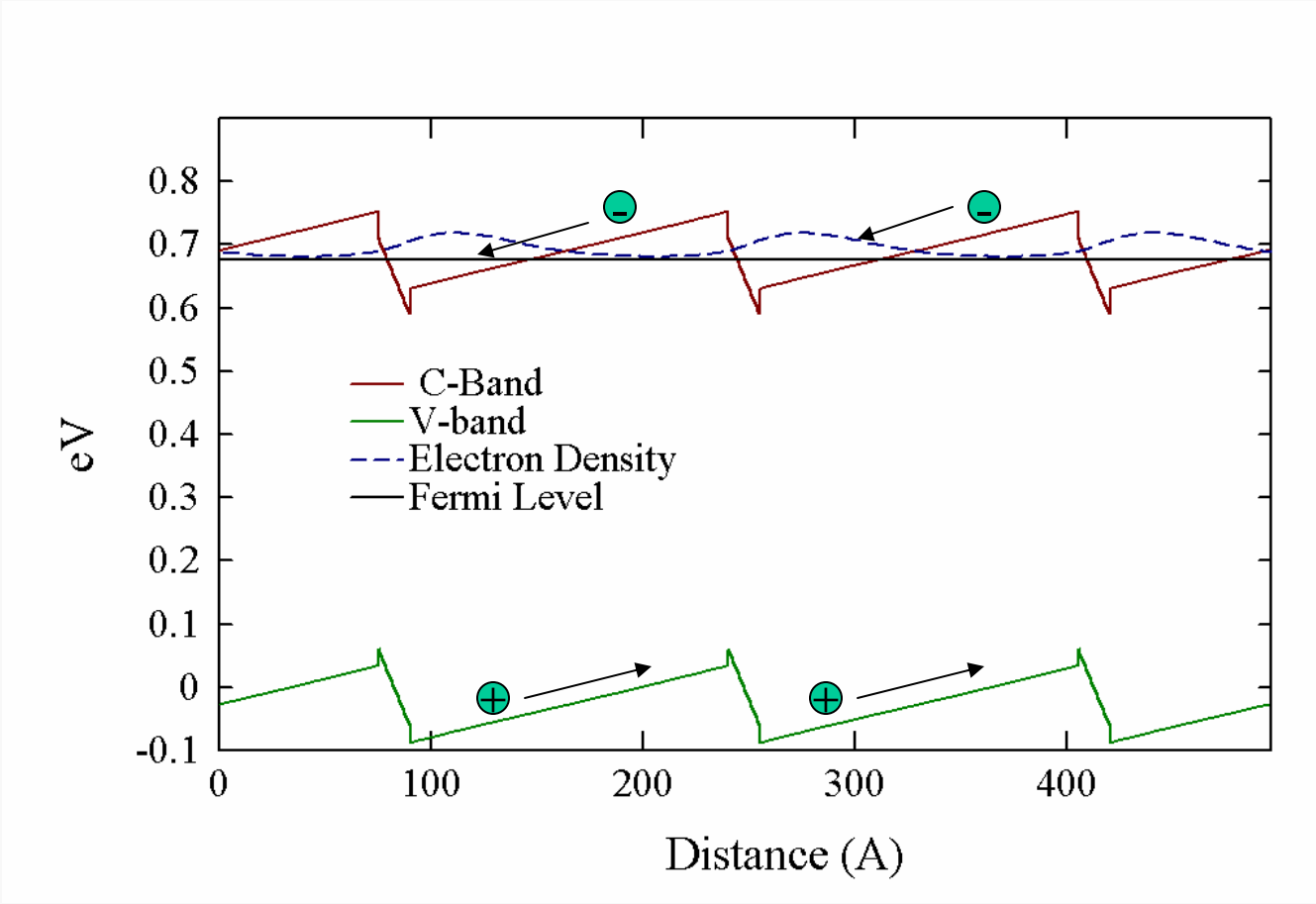

- **Background electron charge localized in triangular potential – less screening of THz**
- **For long wavelength pumping photoexcited electron drift in the barrier region opposes diffusion**

Summary

- There is a strong military need for compact, field deployable THz generation and detection systems with higher efficiency sources
- Fiber-based fs and CW telecom Lasers are attractive, but operate at different wavelength than existing systems
- InN and InN/InGaN quantum wells and photomixers have strong potential for efficient THz emission at 1550 nm using both pulsed and CW approaches.